Scheinberg A., Fu R. R., Elkins-Tanton L. T., and Weiss B. P. (2015) Asteroid differentiation: Melting and large-scale structure. In *Asteroids IV* (P. Michel et al., eds.), pp. 533–552. Univ. of Arizona, Tucson, DOI: 10.2458/azu_uapress_9780816532131-ch028.

Asteroid Differentiation: Melting and Large-Scale Structure

A. Scheinberg and R. R. Fu
Massachusetts Institute of Technology

L. T. Elkins-Tanton
Arizona State University

B. P. Weiss
Massachusetts Institute of Technology

The diversity of mineralogies and textures in the asteroidal meteorite collection promises a similarly diverse array of parent bodies and relatives as we continue exploring the asteroid belt. The presence of metamorphosed and igneous meteorites demonstrates that even some small bodies were heated significantly, permitting a variety of complexly interacting processes and heterogeneities within an individual planetesimal. In particular, chondritic meteorites could even originate from the same parent body as some highly differentiated meteorites. The histories and present-day features of the asteroids depend on their initial composition and the timing and duration of the accretion process. We first discuss the energy sources driving thermal modification of planetesimals and summarize the processes involved in differentiation as hydrous, metal, and silicate melting occurs. Then we outline the aftermath of differentiation as the body cools, and close with a discussion of magnetic, geophysical, and meteoritic evidence for differentiation in planetesimals.

1. ENERGY SOURCES FOR METAMORPHISM AND MELTING

Chondrites consist of material that never heated sufficiently to melt, while primitive achondrites only underwent partial melting. Such samples can be explained as fragments of relatively homogeneous small bodies without invoking differentiation processes. However, iron meteorites analogous to planetary cores and stony achondrites analogous to differentiated planetary crusts demonstrate that metal-silicate differentiation occurred in planetesimals during the first few million years after the formation of calcium-aluminum-rich inclusions (CAIs) (e.g., *Kleine et al.,* 2012; *Markowski et al.,* 2006; *Baker et al.,* 2005).

Differentiation requires heating above the melting temperature of iron-nickel alloys, and may require melting beyond the silicate solidus as well. First melting of bulk chondritic meteoritic material occurs at the Fe,Ni-FeS eutectic at 950°C (*Kullerud,* 1963). Even higher temperatures are probably necessary to facilitate large-scale differentiation (see further discussion in section 2.2).

Two potential heat sources contributed largely to melting in a planetesimal: radiogenic heating from short-lived radioisotopes ^{26}Al and ^{60}Fe (*Fish et al.,* 1960; *Huss et al.,* 2006; *LaTourrette and Wasserburg*, 1998; *Lee et al.,* 1976; *Urey,* 1955) and the gravitational energy of accretion. A third potential source, electromagnetic induction heating (*Sonnett and Colburn,* 1968; *Sonnett et al.,* 1968; *Herbert et al.,* 1991), has received little attention recently, and relies on relatively unconstrained parameters. A better understanding of T Tauri star mass loss has rendered it less plausible as a dominant heat source (*Ghosh et al.,* 2006) and it has not been included in recent thermal models.

1.1. Distribution and Effects of Initial Solar System Aluminum-26

Radioactive decay of the aluminum isotope ^{26}Al into ^{26}Mg is thought to be the primary heat source for planetesimals in the early history of the solar system. The idea was first postulated by *Urey* (1955), who suggested that short-lived radionuclides (SLRs) such as ^{26}Al could have contributed more energy than the primary modern-day contributors to radiogenic heating, ^{238}U, ^{232}Th, and ^{40}K. Heating of a parent body is significantly affected by the initial isotopic abundance of ^{26}Al. Much effort has therefore been expended in measuring meteoritic materials in an attempt to determine the distribution of ^{26}Al in the planetary nebula and in planetesimals.

Most CAIs contained an initial ^{26}Al/^{27}Al ratio near what has been called the "canonical" value, $5.23 \pm 0.13 \times 10^{-5}$ (*Jacobsen et al.,* 2008), derived from bulk CAI measurements in CV chondrites. However, the initial ratio of ^{26}Al/^{27}Al in

individual CAIs is known to have varied from $<2 \times 10^{-6}$ to 5×10^{-5} (*Krot et al.,* 2012). For example, CH chondrites, which are among the most primitive identified, had an initial $^{26}Al/^{27}Al < 5 \times 10^{-6}$ (*Makide et al.,* 2009; *Sahijpal and Goswami*, 1998; *Liu et al.,* 2009; *Krot et al.,* 2008). *Krot et al.* (2012) comprehensively summarized variations in initial ^{26}Al concentrations of CAIs between and within chondrite groups. Rather than a homogenous distribution of initial ^{26}Al at the canonical ratio, meteoritic evidence implies that ^{26}Al was unevenly distributed through the planetary disk.

Primitive materials with very low radiogenic content may have formed before injection of ^{26}Al into the solar system (e.g., *Makide et al.,* 2009; *Liu et al.,* 2009; *Krot et al.,* 2008), or they may have formed after ^{26}Al mostly decayed (*Krot et al.,* 2005; *MacPherson et al.,* 1995). The isotopic ratio is too high to be explained by solar irradiation (*Duprat and Tatischeff,* 2007) and thus must have been exogenous to the solar system. The nature of the stellar source of SLRs is still unsettled, although massive star wind is a good candidate (*Gounelle and Meynet,* 2012). See further discussion in the chapter by Johansen et al. in this volume.

The radiogenic component may have been mixed into the nebula before the formation of a planetary disk, and the planetary disk may have partially homogenized the aluminum composition (*Krot et al.,* 2012). Further homogenization of ^{26}Al distribution may have occurred with radial mixing and accretion, effectively damping the range of compositions from the CAIs samples as they accreted into larger bodies. If this homogenization was not complete, then planetesimals would not be expected to have had identical ^{26}Al compositions. Instead, the ^{26}Al content of a given planetesimal would have depended upon both time and radial domain within the planetary disk of its accretion.

The range of ^{26}Al content within CAIs is large enough to influence whether significant melting will occur. *Kunihiro et al.* (2004) found that there is insufficient radiogenic aluminum in CO and CV chondrites to cause more than minimal melting even with the help of radiogenic ^{60}Fe. However, they assumed that these bodies accreted instantaneously after the age of the youngest chondrules (estimated to be ~2–3 m.y. after CAI formation). In contrast, *Elkins-Tanton et al.* (2011) and *Weiss and Elkins-Tanton* (2013) found that the potentially older age of CV chondrules (the oldest being essentially as old as CAIs) means the CV body could have melted if it started to accrete before the age of the youngest chondrules (i.e., before ~1.5 m.y. after CAI formation).

The canonical ^{26}Al concentration yields an integrated energy output of around $\varepsilon_i = 6.7 \times 10^6$ J kg^{-1} (*Moskovitz and Gaidos,* 2011). If this energy were converted to heat all at once, it would suffice to raise temperatures by several thousand degrees and completely melt the host material. The energy output is derived by integrating over time the power from radiogenic decay

$$\varepsilon_i = \int_0^\infty W \frac{m_{Al}}{m} \frac{^{26}Al}{^{27}Al} e^{-\lambda t} dt \quad (1)$$

where w is heat production for pure ^{26}Al [W kg^{-1}], given by $w = \lambda E_0/m_0$, where λ is the decay constant of ^{26}Al, m_0 is the mass of a single isotope, and E_0 is the energy produced by its decay; (m_{Al}/m) is the bulk elemental mass fraction of Al (approximately the same as solely for the isotope ^{27}Al); and $(^{26}Al/^{27}Al)$ is the isotopic ratio at CAI formation (t = 0).

To obtain the energy output available for heating for accretion times after the time of first formation of solids in the solar system, the initial power is multiplied by $e^{-\lambda t}$, where t is the time from CAI formation to instantaneous accretion. By definition, half the integrated energy output is produced within the first half-life. Therefore, due to its short half-life [0.71 m.y. (*Norris et al.,* 1983)], the effect of ^{26}Al on planetary bodies strongly depends on the timeline of accretion. Radiogenic heating depends on the quantity of material, and therefore is proportional to the radius cubed of a body, while radiative heat loss depends on area, which grows as radius squared. Thus if the bulk of accretion occurred within a million years, the majority of radiogenic heat would have remained in the body; otherwise, it would have readily dissipated.

Given the chondritic abundance of ^{26}Al shown in Table 1, ^{26}Al decay provides sufficiently large amounts of heating that models agree that bodies that accreted to more than ~7–10 km radius before ~1.5 m.y. after the formation of CAIs likely contained sufficient ^{26}Al to melt internally from radiogenic heating (*Hevey and Sanders,* 2006; *Merk et al.,* 2002; *Sahijpal et al.,* 2007; *Urey,* 1955). A summary of papers modeling the internal heating, melting, and differentiation of planetesimals is given in Table 2.

Another potentially important radiogenic element is ^{60}Fe, but it has been difficult to constrain the initial $^{60}Fe/^{56}Fe$ ratio because of the isotope's low abundance in CAIs. Until recently, it was estimated at initial $^{60}Fe/^{56}Fe \sim 1 \times 10^{-6}$ (*Tachibana et al.,* 2006; *Dauphas et al.,* 2008; *Mishra et al.,* 2010). However, recent studies have revised the value downward to $\sim 1 \times 10^{-8}$ (*Tang and Dauphas,* 2012; *Chen et al.,* 2013). With this reduced value, the integrated energy output from ^{60}Fe would have been only 1.2×10^4 J kg^{-1}, insignificant in comparison with ^{26}Al output, although its half-life [2.4 m.y. (*Rugel et al.,* 2009)] is several times longer.

Aluminum-26 and ^{60}Fe behave differently in differentiating bodies. Because aluminum is lithophilic, the formation of a core results in an increased concentration of ^{26}Al in the remainder of a planetesimal. While this does subject the mantle to slightly more heating and higher temperatures than would occur in an undifferentiated body, the concentration of radiogenic heating nearer the surface means that that energy reaches the surface more easily, cooling the planetesimal faster. *Moskovitz and Gaidos* (2011) also point out that silicate melt could form a crust that would be especially enriched in ^{26}Al, further enhancing heat flow (see section 2.3 for further discussion). On the other hand, most ^{60}Fe would proceed to the core and would be the only potentially significant radiogenic heat source of a metal planetesimal shard or stripped core (*Moskovitz and Walker,* 2011).

In summary, ^{26}Al, with its relatively high concentration and short half life, would have been the main driving heat

TABLE 1. Primary short-lived radionuclides and their properties.

Variable	Isotope/Element	Value(s)	Units	Reference
Heat production from decay	^{26}Al	0.355	W kg^{26}Al^{-1}	*Castillo-Rogez et al.* (2009)
	^{60}Fe	0.044*		
Bulk content of CV chondrites	Al	1.8	wt. %	*Lodders and Fegley* (1998)
	Fe	24		
Initial isotopic ratio	^{26}Al/^{27}Al	5.23×10^{-5}	—	*Jacobsen et al.* (2008)
	^{60}Fe/^{50}Fe	1×10^{-8}–1×10^{-6}		*Chen et al.* (2013); *Dauphas et al.* (2008)
Decay constant	^{26}Al	3.0124×10^{-14}	s^{-1}	*Castillo-Rogez et al.* (2009)
	^{60}Fe	9.08×10^{-15}		*Rugel et al.* (2009)

*Derived given w = λE/m, where w is heat production from decay, λ is the decay constant, m is the mass of a single isotope, and E is the energy produced by its decay.

TABLE 2. Chronological summary of selected published asteroid thermal evolution models.

Reference	Model
Urey (1955)	First feasibility calculation of ^{26}Al as an asteroid heat source
Grimm (1985)	Model of asteroid metamorphism with fragmentation and reassembly
Grimm and McSween (1989)	^{26}Al heating model of ice-bearing planetesimals, to account for aqueous alteration in CC
Haack et al. (1990)	Thermal model of a differentiated asteroid based on decay of long-lived radionuclides
Miyamoto (1991)	^{26}Al heating model to account for aqueous alteration in CC asteroids
Grimm and McSween (1993)	Explanation of inferred thermal stratification of the asteroid belt based on heliocentric accretion and ^{26}Al heating
Bennett and McSween (1996)	Updated ^{26}Al heating model for OC asteroids, using revised chronology and thermophysical properties
Akridge et al. (1998)	Model for ^{26}Al heating of OC asteroid [(6) Hebe] with a megaregolith
Ghosh and McSween (1998)	^{26}Al heating model of HED parent body (4) Vesta
Wilson et al. (1999)	Overpressure and explosion resulting from heating CC asteroids
Young et al. (1999)	^{26}Al heating model of CC asteroids with fluid flow, to explain O-isotopic fractionations
Wilson and Keil (2000)	Thermal effects of magma migration in (4) Vesta
Ghosh et al. (2001)	Effect of incremental accretion on inferred thermal distribution of asteroids in the main belt
Merk et al. (2002)	Effect of incremental accretion on internal melting
Hevey and Sanders (2006)	Incorporate silicate melt convection for 64-km body
Sahijpal et al. (2007)	Included ^{60}Fe heating and partitioning during differentiation
Davison et al. (2010)	Heating due to impacts of porous planetesimals
Moskovitz and Gaidos (2011)	Included removal of ^{26}Al in interior due to melt migration
Šrámek et al. (2012)	Compaction and differentiation in bodies 500 km with radius-dependent accretion rates
Neumann et al. (2012)	Compaction and differentiation in initially porous bodies 120 km
Henke et al. (2012)	Sintering in initially porous planetesimals
Golabek et al. (2014)	Three-dimensional finite-element model including parameterized melt convection for the acapulcoite-lodranite parent body

Extended from *McSween et al.* (2002).

source for melting prior to ~2 m.y. after CAIs (e.g., *Merk et al.,* 2002), while ^{60}Fe, with a longer half-life, might have supplied some critical late heating within the core if the first concentration estimates are accurate.

1.2. Effects of Accretion Characteristics and Body Size

Accretionary energy is the potential gravitation energy input released by assembling a body from materials initially at infinite distance

$$E = \int_0^R \frac{G\,M(r)\,dm}{r} \quad (2)$$

where E is accretionary gravitational potential energy [J], G is the gravitational constant, M(r) is the mass of the planet as a function of radius r, expressed as $4/3\pi r^3\rho$ [kg] where ρ is density, and dm can be expressed as $4\pi r^2\rho dr$. This integration yields $E = 16/15\pi^2\rho^2GR^5$. For a planetesimal with a 10-km radius, total accretionary gravitational potential energy E is ~10^{17} J, and for a 300-km-radius body, ~10^{25} J (in comparison, for Earth E is ~2×10^{32} J; for Mars, ~5×10^{30} J; and for Mercury, ~2×10^{30} J).

The addition of energy can be roughly translated to temperature increase using the expression $\Delta T = E/MC_P$, where C_P, the heat capacity, is ~800 J kg^{-1} K^{-1} for silicates (*Fabrichnaya,* 1999) and is only slightly higher for metallic core material (*Bartels and Grove,* 1991). The hypothetical

10-km-radius planetesimal would have been heated only a fraction of a degree if all accretionary energy were instantaneously applied homogenously to the whole body, and the hypothetical body with 300-km radius would have been heated by only 10° to 20°C.

Due to radiogenic heating, these early accreting bodies would have melted from the interior outward, resulting in an interior magma ocean under a solid, conductive, undifferentiated shell (*Ghosh and McSween,* 1998; *Hevey and Sanders,* 2006; *McCoy et al.,* 2006; *Merk et al.,* 2002; *Sahijpal et al.,* 2007; *Schölling and Breuer,* 2009). The size of the body therefore strongly impacted thermal evolution, since heat was being produced in the bulk interior and being radiated from the surface. Other critical controlling parameters are the rate of accretion, the initial ^{26}Al ratio, the initial Al bulk composition, the material density and composition (which control both radiogenic content and heat transfer), and the rate of accretion.

The rate and timing of accretion are highly dependent on the assumed model of planetesimal accretion. In one scenario, sticking collisions between solid particles in the nebula may lead to steady incremental growth of the first planetesimals (*Windmark et al.,* 2012). Alternatively, centimeter- to meter-sized objects may be concentrated by streaming instabilities or by turbulent eddies into 10- to >100-km-sized solid bodies on timescales of just tens to hundreds of years in the asteroid belt region (*Cuzzi et al.,* 2008; *Johansen et al.,* 2007; *Morbidelli et al.,* 2009). For many bodies, this early collapse phase may have been followed by a subsequent period of incremental growth. Turbulent concentration is an inefficient process, owing to disruption of clumps by rotational breakup and ram pressure from the surrounding gas, such that bodies were likely produced sporadically over millions of years (*Chambers,* 2010). Each body would have collapsed quickly, but may have had further coatings added to their surfaces over the tail of accretion as the disk cleared out.

Despite this complexity, most models consider instantaneous accretion over a range of times starting with the age of CAIs. Recent numerical modeling incorporating the effects of prolonged accretion suggests that molten planetesimals can build up substantial (kilometers to tens of kilometers thick) crusts if they accrete to radii of at least a few tens of kilometers by 1.5 m.y. after CAI formation and continue to accrete over a minimum period of perhaps one to several million years (*Sahijpal and Gupta,* 2011; *Elkins-Tanton et al.,* 2011; *Šrámek et al.,* 2012; *Neumann et al.,* 2012; *Weiss and Elkins-Tanton,* 2013).

1.3. Impact-Induced Metamorphism and Melting

Aside from their bulk contribution of accretionary energy, impacts also played a more direct role in metamorphism and melting on planetesimals, although current consensus assigns an uncertain but likely volumetrically minor effect (*Keil et al.,* 1997; *Šrámek et al.,* 2012).

The abundance of metamorphosed ordinary chondrites suggests global-scale metamorphism (e.g., *Wood,* 1962; *Van Schmus and Wood,* 1967; *Dodd,* 1969). *Wasson et al.* (1987), *Cameron et al.* (1990), and *Rubin* (1995) argued for impact-induced heating as the most likely heat source. *Keil et al.* (1997) disfavored this hypothesis after determining, based on laboratory shock wave and cratering experiments and numerical models, that the cumulative global temperature increase due to impacts would be at most a few tens of degrees. However, *Rubin and Jones* (2003) and *Rubin* (2004) presented further evidence of impact heating in meteorites and argued for a major effect of porosity, which although mentioned, was not accounted for in numerical heating models. Most asteroids are believed to have porosities near 30%, although estimates for some range up to 70% (*Britt et al.,* 2002); this would have been even higher in the early solar system before compaction processes (impacts included). *Davison et al.* (2010) accounted for porosity and found that collision of highly porous bodies could in some cases result in nearly global melting. However, they conclude that the cumulative effects of nondisruptive impacts for a typical planetesimal would be minor, with no more than 3% heated by more than 100°C. A final disruptive impact, on the other hand, would melt one-tenth of the parent body.

Ciesla et al. (2013) numerically modeled impacts on porous bodies that were already being heated by ^{26}Al. They concluded that while local heating and metamorphism would occur near the site of the impact, impacts would actually accelerate global cooling of the planetesimal in two ways. First, hot material (primarily heated by ^{26}Al) from deep in the body would be drawn up toward the surface by the impact, leading to a faster cooling rate for this hot material and thus a larger net heat flow rate out of the body. Second, newly compacted material would have a higher thermal conductivity, further enabling heat flow from the body.

Evidence of shock events in meteorites (e.g., *Scott et al.,* 1992; *Sharp and de Carli,* 2006) probably records impact events in the early solar system. However, the contribution of impacts to metamorphism and melting was probably low on a global scale. Subcatastrophic impacts may have even reduced the likelihood of melting by allowing internally heated material to cool more quickly.

2. PLANETESIMAL DIFFERENTIATION PROCESSES DURING HEATING

Based on our current knowledge of their physics and chemistry, planetesimals may have a range of internal structures and material states following peak heating, including an unmelted onion-skin structure, a partially differentiated body with some magma within and a primitive crust, a partially differentiated body with magma that erupted and flooded a primitive crust, and a body that melted entirely (Fig. 1).

Internal radiogenic heating coupled with radiation from the planetary surface means that a planetesimal would initially form an "onion shell" structure, with the highest temperatures reached in its center, surrounded by concentric zones of materials exposed to progressively lower peak temperatures (see *McSween et al.,* 2002, and references therein).

Such a body, should it never reach a melting temperature, is considered primitive, but still could be highly altered from its original, unheated material. Its interior may be variably heated and metasomatized by mobile fluids, and these fluids may be unevenly redistributed within the body, or lost to space, or both. Furthermore, the bulk density of the body may change due to sintering and fluid migration.

Should the interior be heated to the point of melting, a further spectrum of potential planetesimal structures is possible. As temperature rises in a young planetesimal interior, the silicates will pass through the stability zones for several possible hydrated silicate minerals, but then a free hydrous fluid will be released. The first melting to occur will be eutectic melting of iron-nickel sulfide. This metal liquid may or may not be able to migrate downward and form a core without silicate melting.

If accretion is rapid and aluminum remains in the matrix [i.e., it is not all pulled away through buoyant melt migration, as in *Moskovitz and Gaidos* (2011)], then the planetesimal may be rapidly and completely melted and differentiated (e.g., *Hevey and Sanders,* 2006). Vesta itself may be such a body.

Other planetesimals may only undergo *partial differentiation*. In this scenario, the body differentiates internally into a primarily metallic core and a bulk silicate mantle. A chondritic lid would either be retained from original material that never melted, or accreted onto the surface during and after the primary melting phase. Models indicate that in some cases this chondritic lid would be flooded with magma from the interior, while in other cases it would be remain at the surface (*Fu and Elkins-Tanton,* 2014; *Wilson and Keil,* 2012). In either case, a partially differentiated planetesimal would be differentiated internally but retain chondritic material at or near the surface. Multiple meteorite types could therefore be sourced from the same parent body (*Elkins-Tanton et al.,* 2011; *Weiss and Elkins-Tanton,* 2013; *Golabek et al.,* 2014).

In the next three sections, we consider the behavior of volatile, metal, and silicate material, respectively, as they successively melt during the progressive heating of a planetesimal.

2.1. Flow and Escape of Volatile Compounds

For planetesimals accreting with a water ice component, progressive internal heating due to radiogenic decay results in ice melting once temperature surpasses approximately 0°C (Fig. 2). In such a scenario, the formation of liquid water may lead to mineralogical changes that are reflected in the observed

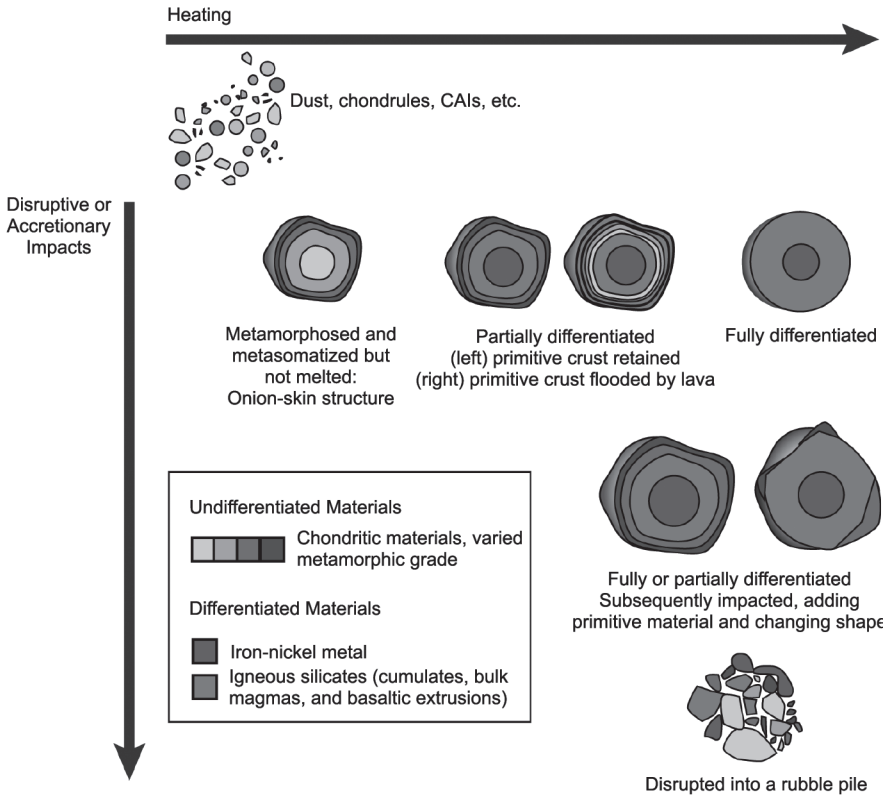

Fig. 1. See Plate 17 for color version. Three possible end-states of asteroid differentiation. *Left:* Unmelted but variably metamorphosed and aqueously altered body composed of chondritic materials. *Middle:* Partially differentiated body with melted interior and unmelted surface layer. *Right:* Fully differentiated body with metallic core and igneous silicate mantle. *Bottom:* Partially or fully differentiated bodies disrupted and coated by later impacts, disrupted even to the point of internal disorganization into a rubble pile.

elemental, isotopic, and modal compositions of meteorites and asteroids. Flow of interstitial water, if it occurred, may have also resulted in the transport of labile elements, altering the local bulk composition in affected regions of the planetesimal. Finally, the presence of water and other volatiles during the melting of the metallic and silicate components of the planetesimal may alter the migration patterns of the resulting melt.

Meteoritic observations indicate that most chondritic parent bodies indeed accreted with significant quantities of water (*Brearley,* 2006). Carbonaceous chondrites include abundant hydrated minerals in addition to free water. The total mass fraction of H_2O measured in highly altered CM and CI chondrites ranges between 0.09 and 0.17 (*Jarosewich,* 1990). Ordinary chondrites typically display lower H_2O abundances of <0.02. However, metamorphism above 200°–300°C leads to the dehydration of silicate phases and removal of H_2O in chondritic material (*Akai,* 1992; *Meunow et al.,* 1995). The high metamorphic grade of most ordinary chondrites, coupled with observations that mildly metamorphosed ordinary chondrites contain hydrated phases (*Alexander et al.,* 1989; *Hutchison et al.,* 1987), suggests that ordinary chondrite parent bodies accreted with significantly higher water content than presently observed, likely greater than 0.02 mass fraction. Metamorphism may also be responsible for the low water contents of dry carbonaceous chondrites. In a well-studied case, the Allende CV chondrite contains no water at the present time while displaying mineral assemblages that strongly imply the past presence of hydrated minerals during a period of fluid-assisted metamorphism (*Brearley and Krot,* 2012; *Krot et al.,* 1997, 1998). Spectroscopic observations of main-belt asteroids confirm the prevalence of hydrated mineralogies (*Jones et al.,* 1990; *Rivkin et al.,* 2002).

The hydration of originally anhydrous phases in chondritic planetesimals commenced shortly after internal heating led to the formation of liquid water. The oxygen and carbon isotopic composition of material from several CM chondrites shows that aqueous alteration occurred between 0° and 70°C (*Clayton and Mayeda,* 1984; *Guo and Eiler,* 2007; *Lerner,* 1995). Meanwhile, altered minerals in CR and CI chondrites likely formed in conditions of <130°C and 50°–150°C, respectively (*Lee et al.,* 1992; *Zolensky et al.,* 1989). Continued heating leads to the decomposition of alteration phases between 200° and 900°C (*Akai,* 1992; *Meunow et al.,* 1992, 1995). Even in the largest, Vesta-sized planetesimals, pressures in the deep interior are unable to stabilize hydrated minerals above ~950°C (*Niida and Green,* 1999). Therefore, progressive interior heating of differentiating planetesimals implies both a hydration and a dehydration phase — free water becomes bonded to secondary, hydrous silicates in the 0°–200°C range and are released again as a free fluid between 200° and 900°C.

The presence of free fluids inside internally heated planetesimals over a wide range of temperatures permits the redistribution of labile elements during fluid flow. For differentiating bodies undergoing progressive heating due to ^{26}Al, the rapid rise in temperature implies that free fluids in most of the interior persist for a timescale of only 0.1–1 m.y. before the onset of metallic and silicate melting (*Fu and Elkins-Tanton,* 2014). The length scale of elemental redistribution during this time period depends on the velocity of fluid advection.

Fluid flow velocities in planetesimals may be modeled by balancing driving forces arising from gravitational and thermal sources with resistive forces arising from the low permeability of chondritic material. The density of liquid and supercritical water at the relevant pressures ranges between 900 kg m^{-3} at 200°C and only 4.5 kg m^{-3} at 900°C (*Smits et al.,* 1994). The large difference between these

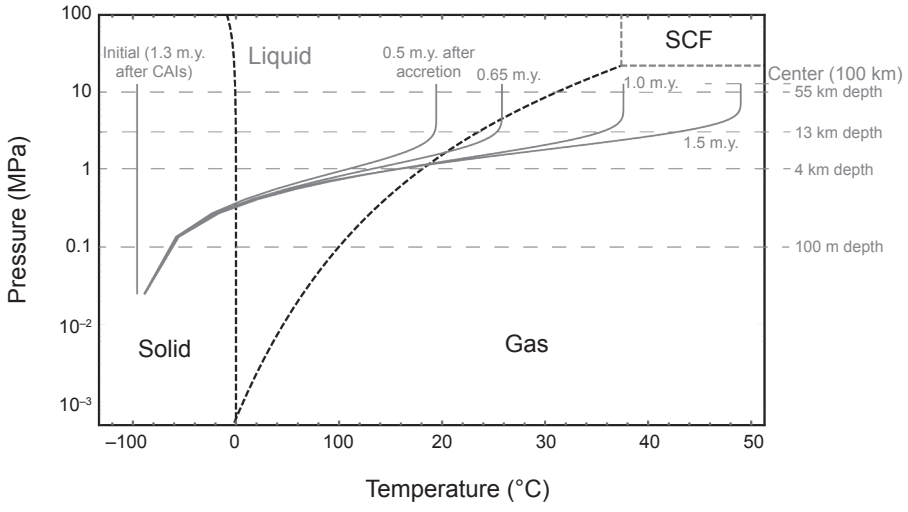

Fig. 2. The evolving temperature profile of an early forming, 200-km-diameter planetesimal internally heated by the decay of ^{26}Al. Temperatures in the body interior are compared to the phase diagram of pure H_2O. Note the formation of gas phase at ~10 km depth during progressive heating. SCF = supercritical fluid.

densities and those of the surrounding chondrite matrix [2100–3700 kg m^{-3} (*Britt and Consolmagno,* 2003)] is one potentially significant driving force, especially after heating above the 374°C critical point of water. The velocity (v_D) of such density-induced Darcy flow is given by (*Bear,* 1972)

$$v_D = \frac{kg\Delta\rho}{\eta\phi} \quad (3)$$

where k is the rock permeability, g is the gravitational acceleration, $\Delta\rho$ is the difference in density between the fluid and rock, η is the dynamic viscosity, and ϕ is the dimensionless volumetric porosity. For a permeability of 10^{-15} m^2 corresponding to permeable carbonaceous and ordinary chondrites [see discussion below and *Corrigan et al.* (1997) and *Sugiura et al.* (1984)], a dynamic viscosity of 5×10^{-5} Pa s (*Sengers and Kamgar-Parsi,* 1984), and a dimensionless porosity of 0.1, fluid is expected to migrate at rates of ~1 m yr^{-1} (*Fu and Elkins-Tanton,* 2014), implying that whole-body fluid flow can occur within the time span of radiogenic heating. Assuming a body radius on the order of 100 km, permeabilities as low as 10^{-16} m^2 would permit the migration of fluids from the deep interior to the surface on 1-m.y. timescales. Migration driven by this mechanism is expected to result in a single pass of fluids from the deep interior to the surface, which has been termed *exhalation flow*. The buoyant fluid may freeze in any conductive lid, after metasomatizing some regions, or it may be lost to space (*Young et al.,* 2003).

In contrast, multiple pass flow of pore fluid due to thermal convection may result from the large vertical temperature gradient in early forming planetesimals. After deriving the convective stability criterion for fluids in an internally heated, radially symmetric body with an equilibrium conductive temperature gradient, *Young et al.* (2003) concluded that, assuming permeabilities of 10^{-13} m^2 (*Grimm and McSween,* 1989), fluids in bodies larger than 120 km diameter would undergo convection.

A major uncertainty in the above fluid transport models is the permeability of chondritic material. Direct measurements on unfractured chondrites have yielded a wide range of permeabilities between 10^{-15} and $<10^{-21}$ m^2, with most measured carbonaceous and ordinary chondrites falling in a range between 0.01 and 2×10^{-15} (*Corrigan et al.,* 1997; *Sugiura et al.,* 1984). The extreme value of $<10^{-21}$ m^2 was obtained from an enstatite chondrite, suggesting that systematic variations in permeability exist between chondrite groups. Models and arguments based on terrestrial analogs have estimated chondritic permeabilities between 10^{-11} m^2 (*Grimm and McSween,* 1989) and 10^{-19} m^2 (*Bland et al.,* 2009). These estimates represent lower bounds on the permeability of bulk material, as fractures may increase the effective permeability by 2 to 9 orders of magnitude (*Brace,* 1980; *Trimmer et al.,* 1980). Furthermore, increasing the relevant length scale from hand sample to kilometers may augment permeability by another factor of 10^3 (*Clauser,* 1992). Observations of chondrite samples reveal a high degree of fracturing and brecciation while the production of gas and supercritical fluids can overcome the tensile strength of chondritic material and lead to fracturing in the deep interior (Fig. 2) (*Grimm and McSween,* 1989; *Young et al.,* 2003). Fractures therefore likely had a significant effect on the permeability of strongly heated planetesimals. Integrating these constraints, for fractured carbonaceous and ordinary chondrite material at the global scale, most permeabilities were likely greater than 10^{-14} m^2, while enstatite chondrite materials may have had permeabilities $<10^{-16}$ m^2, depending on the effect of fractures. The permeabilities for carbonaceous and ordinary chondrites were likely sufficient to permit the planetesimal-scale ascent of fluids (*Fu and Elkins-Tanton,* 2014). In contrast, in the case of parent bodies with low permeabilities of $<10^{-16}$ m^2, fluid-facilitated elemental redistribution may have occurred on only the <100-μm scale (*Bland et al.,* 2009).

The large observed spread in oxygen isotopic composition in the altered components of carbonaceous chondrites provide meteoritic evidence in favor of large-scale fluid migration (*Young,* 2001; *Young et al.,* 1999). The expected heterogeneity in a small volume of water trapped in pore space appears insufficient to explain the isotopic variation, while open-system fluid flow down a temperature gradient is capable of reproducing the measured oxygen isotopes. On the other hand, the essentially solar abundance of elements in CI chondrites (*Lodders,* 2003) and the depletions of volatile elements in other chondrites (*Kallemeyn and Wasson,* 1981) have been cited as evidence against open-system behavior of planetesimal fluids (*Bland et al.,* 2009). However, because most volatile elements are also the most labile, the depletion patterns in carbonaceous chondrites have also been interpreted to be a consequence of open-system fluid flow (*Matza and Lipschutz,* 1977; *Young et al.,* 2003).

To summarize, abundant meteoritic and spectroscopic evidence shows that early forming planetesimals accreted with a significant budget of H_2O and other volatiles. Progressive heating of differentiating planetesimals above ~200°C generated free fluids in the liquid, gas, and supercritical phases. For probable values of permeability in fractured carbonaceous and ordinary chondrite parent bodies, heated fluids were likely able to participate in single-pass exhalation flow and multiple-pass thermal convection in regions with a high temperature gradient. Depending on the degree of fracturing, enstatite chondrite parent bodies may have insufficient permeability to permit large-scale fluid flow.

2.2. Metal Fluid Flow and Core Formation

In order to form a core, the dense melted metal must be able to drain to the body's center and displace the lighter silicate material present there. Although melting of core-forming material likely began when temperatures reached the Fe,Ni-FeS eutectic at 950°C (*Kullerud,* 1963), the core-formation process was complicated by the necessity of pore connectivity, slow adjustment of the silicate matrix, and the presence of volatiles.

The threshold for connectivity of molten Fe-S in an olivine matrix has been estimated as low as 3–6% melt (*Yoshino*

et al., 2003, 2004) but as high as 17.5% (*Bagdassarov et al.,* 2009). An even smaller percent melt is needed when the dihedral angle between the molten metal and solid silicate is less than a critical value of 60°. *Terasaki et al.* (2008) found dihedral angles below 60° for pressures of 2–3 GPa, depending on the liquid's oxygen content. The volume fraction of metal in primitive chondrites typically varies from a few percent to <20% (*Scott et al.,* 1996a), while Earth's metal core is about 15% of its volume. Silicate melting was thus probably unnecessary to reach the connectivity threshold for most planetesimals.

Additionally, the silicate material must have a sufficiently low viscosity that it can be deformed and displaced. If this process is inefficient, then significant differentiation could occur only after partial or complete melting of the silicate, which would occur between the solidus and liquidus temperatures, around 1100°C and 1500°C respectively for planetary silicates (*McKenzie and Bickle,* 1988; *Agee,* 1997). An experimental study by *McCoy et al.* (1999) concluded that significant (~50%) silicate melting, reached at ~1450°C, is necessary to initiate migration of metallic melt in an enstatite chondrite.

However, *Šrámek et al.* (2012) noted that percolation through a solid silicate matrix would proceed on a timescale inversely proportional to length scale and thus would not be observable in a laboratory setting, where length scale is on the order of 1 cm rather than 100 km. The timescale is also inversely proportional to gravity, which scales with radius in a homogenous body. The larger the body, the more quickly this process could occur. This would only be one factor that makes a larger body differentiate faster; more directly, a larger body would reach higher interior temperatures and thus partially melt more readily.

Finally, as discussed in the previous section, volatile elements were likely still present at this stage of heating either as free fluids or as hydrous silicate phases (*Fu and Elkins-Tanton,* 2014). The resulting oxygen fugacity may result in oxidized iron, which could then only be reduced to a metal and flow to form a core after further heating and removal of oxidizing agents through fluid migration. Thus the presence of volatiles may delay metal melting and lead to an overall reduction in melt available for core formation.

Ghosh and McSween (1998) modeled differentiation of the asteroid (4) Vesta (mean radius 263 km) and determined core formation was not possible if accretion (assumed instantaneous) occurred later than 3 m.y. after CAI formation, and that core formation would occur effectively instantaneously at around 4.6 m.y.

Šrámek et al. (2012) modeled the liquid percolation and silicate compaction process for a body heated by ^{26}Al decay and impacts and assumed accretion occurred gradually rather than instantaneously. They considered a multi-phase model tracking metal and silicate material in both solid and liquid form and found that partial melting of silicate is necessary for compaction of the remaining silicate to occur on the planetesimal timescale. They conclude that due to the similar timescales of accretion and radiogenic heating, diverse outcomes are possible depending on size and accretion rate. Bodies with radii of 500–1000 km, if accreted steadily over the first 3 m.y. of solar system history, could have retained enough heat to segregate about half of its metal component, although only half of that (about a quarter of the total metal content) would have formed a core. On the other hand, accretion within 1 m.y. of a 1500-km body would have easily produced a large core. Even a body of this size would not have been able to form a core if accretion were extended over 5 m.y. (about seven ^{26}Al half-lives).

Neumann et al. (2012) considered differentiation of planetesimals with radii smaller than 120 km. Their model included heat loss due to transport toward the surface by silicate melt and found this process would diminish planetesimal heating by tens to 100 K. They found that the core-formation process would have lasted for 2–10 m.y., but that core formation would only be likely if the bulk of accretion occurred within 3.5 m.y. of CAI formation. Porosity played a large role, with the maximum reachable temperature much higher for porous bodies than for comparable consolidated ones. This was especially true for small bodies.

Another scenario for core formation involves the accretion of already differentiated iron-nickel. This would occur when a separate differentiated body or a fragment of one impacted the planetesimal. In this case, the metal could descend as a diapir due to its gravitational instability (e.g., *Stevenson,* 1981; *King and Olson,* 2011). Of course, this can only occur if diffusion through silicate melting or metal melt percolation, as described as above, occurred to differentiate the earlier body. Since the magnitude of the gravitational instability is proportional to gravity and thus radius, it is more likely to occur on larger, planet-sized bodies than on small, early bodies.

2.3. Silicate Transport Effects on Core Formation

An important recent direction in planetesimal modeling involves the role of silicate melt transport in the time evolution of a planetesimal's thermal profile. As the silicate portion begins to melt, this melt may rise buoyantly and depart its source region. *Moskovitz and Gaidos* (2011) argue that because aluminum is preferentially partitioned into the melt phase, the melting source will immediately be depleted in the ^{26}Al heat source, and melting will cease. The rising, ponding melt, however, will heat up even more vigorously due to its concentrated aluminum content. Migration and concentration of ^{26}Al into a crust results in remelting of that crust for accretion times less than 2 m.y. and for bodies >100 km in size.

They also find that subsequent heating from the decay of ^{60}Fe generates melt fractions in excess of 50%, thus completing differentiation for bodies that accreted within 2 m.y. of CAI formation. However, as discussed in section 1.1, these results are based on the larger ^{60}Fe abundance estimates available in the literature at that time but later revised downward by nearly 2 orders of magnitude: This component of heating is probably overestimated.

The *Moskovitz and Gaidos* (2011) result differs slightly from one-dimensional models, in that they find differentiation would be most likely for planetesimals with radii larger

than 10 km that accreted within approximately 2.7 m.y. of CAI formation; the inclusion of ^{60}Fe lengthens the possible time of differentiation from its former ~1.7–2 m.y. after CAIs (*Hevey and Sanders,* 2006; *Elkins-Tanton et al.,* 2011). *Neumann et al.* (2014) pursued a similar scheme in which ^{26}Al is partitioned heavily into the melt phase. In a model for Vesta, a magma ocean 1 km to a few tens of kilometers in thickness forms in the near subsurface, as long as accretion occurred before 1.5 m.y. after CAIs. The magma ocean lasts 10,000–1,000,000 yr, and a basaltic crust is extruded onto the surface. Core formation is complete within ~0.3 m.y., and silicate melt is present in the mantle for up to 150 m.y.

Both aluminum sequestration, as investigated by *Moskovitz and Gaidos* (2011) and *Neumann et al.* (2014), and the formation of an early basaltic crust rely on relatively efficient melt migration within these small bodies. *Moskovitz and Gaidos* (2011) point out that melt-migration rates are independent of planetesimal size, since the lower gravity of smaller planetesimals is offset by the shorter distances the melt needs to migrate. Migration on any planetesimal, however, requires that the melt be buoyant with respect to its country rock. In the following section we discuss the buoyancy of melt in putative parent bodies.

2.4. Silicate Melting and Magma Migration

As temperatures continue to climb after the first eutectic melting of Fe,Ni-FeS-rich fluids at 950°C, the first silicate melts appear at 1050°–1150°C while complete melting occurs by 1500°C (*Agee,* 1997; *Agee et al.,* 1995; *McCoy et al.,* 2006). The potential upward migration of these silicate melts may strongly influence the observable surface composition of the body, the style and rate of heat loss (*Neumann et al.,* 2012), the distribution of heat-producing isotopes (*Moskovitz and Gaidos,* 2011; *Neumann et al.,* 2014), the loss of silicate material to space, and the preservation of the primitive chondritic crust.

The direction and rate of silicate melt migration depends on the buoyancy of the magma relative to the overlying unmolten chondritic lid. The abundance of volatiles is an important control on buoyancy as their presence during silicate melting may lead to exsolution, which would dramatically lower the bulk density of the resulting magma. As discussed in section 2.1, high-temperature fluids on both carbonaceous and ordinary chondrite parent bodies were likely able to ascend efficiently from the deep interior before the onset of silicate melting.

In addition to water, other volatiles, principally CO, CO_2, N_2, and Cl, may have been present in sufficient quantities in chondritic protoliths to potentially affect the density of silicate melts. However, among these volatiles, only CO and Cl are retained in the protolith up to ~1250°C, which is the temperature necessary for efficient silicate melt migration (*McCoy et al.,* 1997; *Meunow et al.,* 1992, 1995). Carbon monoxide is likely present in insufficient quantities (<100 ppm) during silicate melt migration to affect melt densities, except in cases where it is produced by the C-FeO smelting reaction (*McCoy et al.,* 1997; *Wilson et al.,* 2008). Meanwhile, the residual Cl content of chondrites at 1250°C is likely soluble in silicate magmas at low pressures and would therefore not strongly decrease the magma density via exsolution (*Fu and Elkins-Tanton,* 2014; *Webster,* 1997).

Volatile-depleted (dry) melts of ordinary chondrites have model densities similar to those of an overlying fractured lid built from ordinary chondrites. Dry partial melts of carbonaceous and enstatite chondrites are likely denser and lighter, respectively, than a fractured lid with the corresponding composition (Fig. 3) (*Fu and Elkins-Tanton,* 2014; *Jurewicz et al.,* 1993, 1995; *McCoy et al.,* 1999). For parent bodies of CV chondrite composition, which are relevant to the paleomagnetic constraints discussed later in section 4.2, an unsintered, fractured crust would have a density between ~2600 and 2900 kg m^{-3}, whereas the density of molten CV chondrite over a range of temperatures and pressures is between ~2800 and 2900 kg m^{-3}. Therefore, if melts remain volatile poor, silicate magma produced at depth in planetesimals with carbonaceous chondrite compositions are expected to remain in the interior while similar melts on enstatite chondrite parent bodies likely ascend to the surface. Ordinary chondrite parent bodies represent an intermediate case where the fate of silicate magmas depends on the macroporosity of the overlying lid.

Some chondritic parent bodies may retain sufficient volatiles to result in exsolution-driven melt ascent. In the case of enstatite chondrite parent bodies, low bulk permeability may lead to the retention of H_2O at depth (see section 2.1).

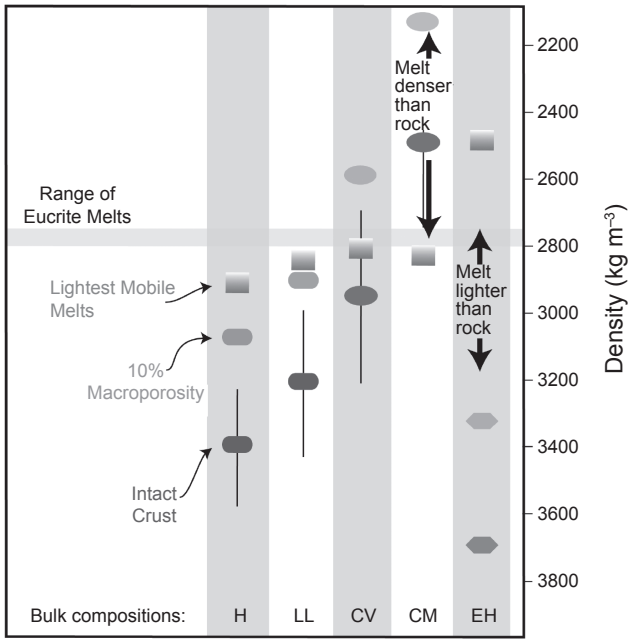

Fig. 3. Comparison of the densities of mobile silicate melts and unmolten chondritic material for five meteorite groups. Intact crust densities and uncertainties represent the measured densities of chondrite hand samples, while the values with 10% macroporosity approximate the bulk densities of fractured chondritic lids. Reproduced from *Fu and Elkins-Tanton* (2014, *EPSL*) with permission of Elsevier.

Likewise, carbonaceous and ordinary chondrite parent bodies with low intrinsic permeability, low degree of fracturing, or high initial volatile contents may have generated sufficiently volatile-rich melts to undergo buoyant ascent.

In such scenarios, magmas forming inside planetesimals may be expected to erupt with force, driven by expanding volatiles (*Muenow et al.,* 1992, 1995; *Wilson and Keil,* 2012). Melt extraction from the partially molten interior likely occurred in two stages (*Wilson et al.,* 2008; *Wilson and Keil,* 2012). First, magma would have ascended in dikes, but flow rates were likely insufficient to sustain continuous eruption from the melting region directly to the surface. This was especially the case for parent bodies smaller than ~400 km in diameter. The ascending melt therefore collected in sills within the chondritic lid. Second, the melt in these magma chambers, especially if it was volatile rich, would have explosively erupted onto the surface, propelling silicate fragments up to 1 m in size beyond the escape velocity of small (<100-km-diameter) asteroids (*Wilson and Keil,* 1991; *Wilson et al.,* 2010). On larger bodies with stronger gravity, most erupting melt may have been retained on the surface in melt ponds that, with sufficient accumulation, led to the subsidence and destruction of the primitive chondritic lid (*Wilson and Keil,* 1997, 2012).

Ghosh and McSween (1998) describe an end-member model for Vesta in which all melt from the interior erupts onto the surface and another end-member model in which no melt extrudes; their efforts demonstrate the difficulty of arguing completely for one or another eruptive scenario.

In summary, the potential of silicate melts to ascend from the melting region depends critically on the persistence of volatiles at supersolidus temperatures and on the parent body's bulk composition. Volatile-rich melts, which may have formed on bodies with very low fluid permeabilities such as enstatite chondrite parent bodies, are expected to rise efficiently to the surface, potentially resulting in the inundation of the chondritic lid and ejection of mass from the parent body. The discovery of possible pyroclasts of aubritic composition such as Larkman Nunatak (LAR) 04316, which may be sourced from an enstatite-chondrite-like protolith, supports the hypothesis that enstatite chondrite parent bodies retained sufficient volatiles to drive magma ascent (*Keil,* 2010; *Keil et al.,* 2011). For differentiated planetesimals with carbonaceous and ordinary chondrite compositions, efficient release and upward transport of volatiles before the onset of silicate melt migration likely resulted in negatively buoyant melts that permitted the preservation of the primitive chondritic lid on these bodies.

3. COOLING AND SOLIDIFICATION OF PLANETESIMALS

3.1. Solidification of a Partially Molten Silicate Mantle

The physical process of magma solidification influences the range of both composition and texture that will occur in the mantle and possible crust of a planetesimal. The compositional process of solidification can be viewed as having two end members: fractional solidification and batch solidification (e.g., *Solomatov,* 2000). For fractional solidification to occur, mineral grains must settle from flow and be effectively removed from communication with the remaining magma ocean liquids. The residual liquid composition thus evolves with the progressive removal of solidified material. In batch solidification, liquid contact and equilibrium are maintained throughout solidification. A fractional solidification model of a magma ocean therefore predicts mineral assemblages, cumulate bulk composition, and cumulate trace-element compositions that are completely different from those occurring in equilibrium solidification.

Due to their relatively small masses, planetesimals have internal pressures so low that, once melted, the bottom of a planetesimal's magma ocean has effectively the same pressure as the top. The high-pressure gradient in planets the size of Earth likely encourages fractional solidification as cool downwellings from the surface develop crystallinity with depth and deposit crystals at the bottom boundary. Without significant pressure or gravity, magma oceans on planetesimals may not fractionally solidify. Over the ~0.5-kbar mantle pressure range of a planetesimal ~200 km in radius, the solidus will change by only about 10°C, and the adiabat by only ~2°C. As it cools, therefore, the entire depth of the magma ocean will contain some crystal fraction. The magma ocean will have a high effective viscosity, perhaps in the range of hundreds to thousands of Pascal seconds. Combined with the high heat flux of a small body cooling without an atmosphere, mineral grains would have to be large, perhaps several to 10 cm, to settle from the magma ocean. Thus, in the time before crystallinity rises, only the earliest-forming crystals will settle (*Suckale et al.,* 2012). Given almost any of the candidates for bulk-chondritic silicate compositions and the low pressures in planetesimals, olivine alone would be the first material to crystallize. The rest of the planetesimal's mantle will solidify in bulk and never produce an olivine cumulate. This may be why we have no such samples in our collections.

Despite the lack of meteoritic olivine cumulate samples, olivine is by far the predominant silicate represented in the stony-iron meteorite group known as pallasites. Apart from olivine and metal, main-group pallasites contain <1 vol.% each of chromite, pyroxene, and phosphates (*Buseck,* 1977; *Ulff-Møller et al.,* 1998). Pallasites are usually thought to be samples of a core-mantle boundary (e.g., *Mittlefehldt et al.,* 1998; *Benedix et al.,* 2014), although *Tarduno et al.* (2012) argue instead that pallasites are the result of an impact that injected iron from the impactor's core into a planetesimal mantle. Assuming they are samples of a core-mantle boundary, the simplicity of the mineral assemblages in pallasites and iron meteorites strongly supports successful crystal settling of olivine alone at the beginning of magma ocean solidification in an internally differentiated planetesimal. Later solidification would occur in bulk, and thus planetesimal magma oceans will not produce olivine + pyroxene cumulate,

as predicted for the Moon, but would produce melt extraction from mushes consistent with observations from Vesta.

The slowness of magma movement and the inefficiency of mixing on planetesimals not only makes the formation of olivine cumulates unlikely, it predicts that planetesimals' mantles and crusts may well be inhomogeneous. The accreting material is not likely to be compositionally homogeneous, and it may not efficiently melt and mix. This prediction is supported by the findings of *Kleine et al.* (2012), who find that four texturally and temporally resolved groups of angrites can be identified that were derived from at least two distinct mantle sources. These mantle sources are the result of separate events of core formation, both of which took place within ~2 m.y. of CAI formation. Thus, core formation in the angrite parent body did not occur as a single event of metal segregation from a global magma ocean, but rather took place under varying conditions by several more local events. The disparate Hf-W systematics of the two distinct angrite source regions indicate that convection in the magma ocean was inefficient in homogenizing the composition of the mantle, possibly as a result of a continuous bombardment with small planetesimals during ongoing core formation. Furthermore, they find that mantle differentiation occurred at ~3.6 m.y. after CAI formation, in line with cooling models following early ^{26}Al melting in the parent body.

In summary, the taxonomy of possible internal structures is not limited to the processes of melting. Mantle heterogeneities caused by a small extent of olivine settling followed by batch solidification, as well as complications from melt percolation and mixing caused by continued accretion, probably also influenced planetesimal structure. The surface of the body may experience ongoing accretion of primitive material while the partially or wholly molten interior continues to cool and differentiate. Finally, later impacts may partially strip the body and then allow blocks of material to fall back onto the surface, or may even break the body into pieces and produce a rubble pile.

3.2. Solidification of a Planetesimal Core

Metallic cores would have initially been entirely molten. The temperature at which core crystallization began depends on its composition, in particular, its sulfur content. The liquidus in an Fe-FeS system decreases from 1538°C for pure Fe to 988°C at its eutectic composition (~31 wt.% S), at which point FeS begins to crystallize as well (*Kullerud and Yoder,* 1959). In some parent cores, sulfur content as high as 17 wt. % has been inferred (*Chabot,* 2004). Iron sulfide is far less abundant in the meteorite collection than predicted by models, although this may be explained by the mineral's low strength (*Kracher and Wasson,* 1982; *Chabot and Drake,* 2000).

Although batch solidification might be expected given the shallow pressure gradient and low gravity, concentration trends of various minor and trace elements (e.g., Ni, Au, Ga, Ge, O, P, Ir) in iron meteorite groups demonstrate that their initially molten parent cores underwent fractional crystallization. However, scatter in these element trends indicate that at some point the assumption of a well-mixed liquid broke down (*Haack and Scott,* 1992, 1993; *Pernicka and Wasson,* 1987; *Scott et al.,* 1996b; *Wasson,* 1999; *Wasson and Richardson,* 2001; *Benedix et al.,* 2014).

On large planets, high-pressure gradients result in the adiabatic gradient intersecting the solidus at the body's center, causing solidification to first occur at the body's center and produce a solid, growing inner core. For pressures lower than ~4 GPa, the core-mantle boundary would be the first location to reach the liquidus during cooling (*Williams,* 2009). However, due to the low-pressure gradient in a planetesimal, both the adiabatic gradient and the pressure-induced solidus change in a well-mixed core were very small, with perhaps a ~1°C increase from the core-mantle boundary to the center for an asteroid with a 100-km radius. Because this variation in liquidus is so small, particularly compared to sulfur effects, it is difficult to predict how solidification would have proceeded. *Chabot and Haack* (2006) and *Goldstein et al.* (2009) provide recent reviews of the scenarios and supporting evidence.

Four possible core solidification scenarios are (1) outward concentric crystallization (similar to Earth), (2) inward concentric crystallization, (3) inward dendritic growth, and (4) cumulate solid inner-core formation (Fig. 4). None of these scenarios can be decisively confirmed or rejected on the basis of current observation and evidence.

Sulfur is almost fully excluded from crystallizing iron (*Willis and Goldstein,* 1982). Since increasing sulfur content lowers the melting temperature, a solidification front is inhibited as local sulfur content becomes too high to efficiently diffuse. This likely results in dendritic growth inward from the core-mantle boundary as cooling and solidification continue (*Haack and Scott,* 1992). Although kilometer-sized dendrites have been proposed (*Narayan and Goldstein,* 1982), the dendrites could be gravitationally unstable and descend to form a cumulate inner core. On the other hand, if sulfur accumulates near the core-mantle boundary due to its low density and effectively inhibits crystal growth there, solidification would then occur throughout the core in the form of iron snow. While this has not been discussed in a planetesimal context, iron snow has recently been discussed in the context of the small lunar (e.g., *Laneuville et al.,* 2014) and Ganymede (e.g., *Christensen,* 2015) cores.

These different core scenarios would result in different configurations in modern-day asteroid cores (Fig. 4). An inward-crystallizing concentric solidification front would have the bulk of its late-stage solids (e.g., troilite), which would have formed upon eventually reaching a eutectic Fe-S composition, sequestered in the body's inner core. A dendritic inward-crystallization scenario would show a complicated network of dendrite growth interspersed with light-element-rich pockets. A core that crystallized from the inside out would have an outer core rich in late stage solids. Outward growth through snow or dendritic collapse would have a similar configuration, although inefficient compaction could result in pockets similar to the inward-dendritic-growth scenario.

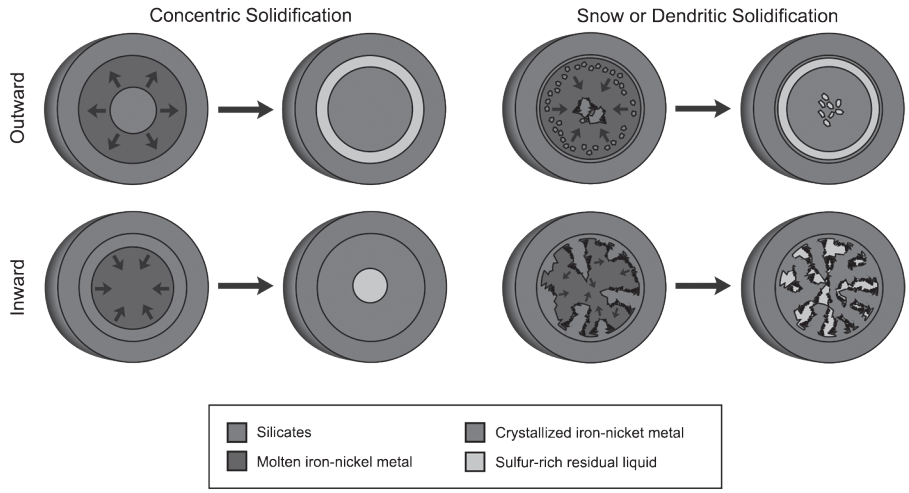

Fig. 4. See Plate 18 for color version. Four possible core solidification scenarios and potentially resulting end-states. *Top left:* Outward (Earth-like) solidification. *Bottom left:* Concentric inward solidification. *Top right:* Outward solid core growth due to accumulated iron "snow" and/or destabilized dendrites. *Bottom right:* Dendritic inward solidification.

4. ASTEROID AND METEORITE RECORDS OF THE DIFFERENTIATION PROCESSES

We have a diversity of geochemical and geophysical constraints on the compositions of asteroid surfaces and interiors. Collectively, these datasets provide evidence for surface compositions ranging from apparently chondritic bodies to fully differentiated bodies and possibly also including partially differentiated bodies. Here we review evidence for asteroidal cores from asteroidal shapes, and then discuss two relatively recently acquired datasets that constrain asteroidal differentiation and large-scale interior structures: studies of the remanent magnetization of meteorites, and *in situ* magnetic field observations of asteroids. These observations detect asteroid remanent magnetization, which in turn likely point to a convecting metal core capable of dynamo action in early solar system history.

4.1. Asteroidal Shape and Core Detection

Absorption and emission spectra acquired in wavelengths from the ultraviolet to the far-infrared constrain the mineralogical and elemental composition of the surface layers of asteroids (see the chapters by DeMeo et al., Masiero et al., Reddy et al., and Vernazza et al. in this volume). Albedo and polarimetry data also provide indirect constraints on surface-layer mineralogy. Radar data constrain the bulk density of the surface layer (see the chapters by Benner et al., Delbo et al., Margot et al., and Scheeres et al. in this volume). Gravity data acquired either from spacecraft encounters, binary asteroid orbits, or perturbations to the orbits of more distant bodies constrain asteroid masses (see the chapter by Scheeres et al. in this volume). When combined with shape data obtained from resolved images and/or joint infrared and optical photometry, the bulk asteroid density and sometimes the interior mass distribution can be constrained (see the chapter by Russell et al. in this volume). For example, the high surface density (ranging up to ~6 kg m^{-3}) of several M-type asteroids strongly suggests they are largely metallic bodies (*Shepard et al.,* 2010), probably derived from early differentiated planetesimals whose silicate mantles were catastrophically removed by a collision (*Asphaug,* 2010).

Spacecraft-based geophysical observations of main-belt asteroids provides evidence for differentiated internal structure. One such example is the asteroid (21) Lutetia, whose high density strongly suggests that its deep interior underwent substantial heating and sintering. Because its surface spectral properties are most similar to those of carbonaceous or enstatite chondrites (*Coradini et al.,* 2011; *Vernazza et al.,* 2011), Lutetia may represent the first known partially differentiated asteroid (*Weiss et al.,* 2012). *Formisano et al.* (2013) find that partial differentiation is likely in scenarios in which Lutetia completed its accretion in less than 0.7 m.y. from the injection of ^{26}Al in the solar nebula and for post-sintering values of macroporosity not exceeding 30 vol.%.

There is indirect evidence for a metallic core in asteroid (4) Vesta from the oblateness of its gravity field and its bulk density (*Russell et al.,* 2012). At the same time, observation of asteroid shape can offer further constraints on the degree of interior melting during the body's early history. Finite-element models of Vesta indicate that, even in the low-gravity regime of such bodies, strong internal heating resulted in a thin early lithosphere that experienced pervasive fracturing, permitting efficient relaxation of the body to a

closely hydrostatic figure (*Fu et al.,* 2014a). Topography data provided by the Dawn spacecraft, combined with derived crustal thickness maps (*Ermakov et al.,* 2014), suggest that a large region in the northern hemisphere of Vesta has escaped significant reshaping due to late giant impacts and preserved an ancient figure closely consistent with an oblate ellipsoid of rotation, which is the shape expected for a body that nearly reached hydrostatic equilibrium. The presence of such a hydrostatic terrain confirms that the entire vestan interior, with the exception of a lithosphere of up to several tens of kilometers in thickness, underwent intense heating above approximately 800°C, which is necessary to permit viscous relaxation on the relevant timescale of asteroid thermal evolution. Future high-resolution observations of other large asteroids, including (2) Pallas, may reveal the presence of analogous hydrostatic terrain and thereby constrain the degree of early interior heating.

4.2. Paleomagnetism of Meteorites

Remanent magnetization is the semipermanent alignments of electron spins in ferromagnetic minerals and provides a record of the intensity of past magnetic fields. It can be acquired by asteroid materials in the form of thermoremanent magnetization (produced during cooling) or as crystallization-remanent magnetization (produced during crystallization) when these processes occur in the presence of a magnetic field. Asteroidal materials could be remagnetized either on their parent body or, for chondrules and refractory inclusions, when they formed as free-floating objects in the nebula (*Weiss and Elkins-Tanton,* 2013). It is also possible that previously magnetized materials could be aligned by a background field as they accreted onto a planetesimal to produce accretional detrital-remanent magnetization (*Fu and Weiss,* 2012).

By constraining the existence and intensity of ancient magnetizing fields, remanent magnetization can be used to infer the existence and nature of putative magnetic field sources in the early solar system. Proposed field sources are magnetism in the solar nebula (dragged in from the parent molecular cloud and/or generated by *in situ* fluid motions), induction currents generated in advecting planetesimal metallic cores (dynamos), and currents transiently generated by impact-produced plasmas (*Weiss et al.,* 2010a). Of these three field sources, only dynamo fields are generated by internal geophysical processes and would therefore place direct constraints on planetesimal differentiation and thermal evolution.

Paleomagnetic studies over the last five decades have found that many chondrites and achondrites contain remanent magnetization. However, until recently, the origin of this magnetization has been unclear. Over the last decade, a burst of measurements (Fig. 5) combined with a deepening understanding of meteoritics and the fundamentals of rock magnetism and dynamo theory has led to major advances in our understanding of meteorite magnetism. Paleomagnetic analyses have identified remanent magnetization in angrites and howardite-eucrite-diogenite (HED) meteorites, two groups of basaltic achondrites (*Fu et al.,* 2012; *Tarduno and Cottrell,* 2012; *Weiss et al.,* 2008), and main-group pallasites (*Tarduno et al.,* 2012). The slow cooling rates experienced by these meteorites through the Curie points of their ferromagnetic minerals on their parent bodies [e.g., at least thousands of years for the angrite Angra dos Reis and the eucrite Allan Hills (ALH) A81001] are inconsistent with impact-generated plasmas as the field source, which are only thought to persist at most for ~1000 s on asteroidal bodies (*Fu et al.,* 2012). The relatively young age of magnetization in these bodies (i.e., <4.557 Ga for Angra dos Reis and 3.69 Ga for ALH A81001) likely excludes magnetic fields in the solar nebula. By comparison, consideration of the physics of dynamo action on planetesimals suggests that magnetic fields could persist on these bodies on timescales ranging from several million years (*Sterenborg and Crowley,* 2013) up to ~200 m.y. after the formation of CAIs (*Elkins-Tanton et al.,* 2011; *Tarduno et al.,* 2012; *Weiss et al.,* 2008). Therefore, it was concluded that all three parent bodies generate dynamo magnetic fields.

Paleomagnetic analyses of the Allende CV carbonaceous chondrite have identified a unidirectional magnetization blocked up to 290°C in bulk samples (*Butler,* 1972; *Carporzen et al.,* 2011; *Nagata and Funaki,* 1983) and some chondrules (*Fu et al.,* 2014b; *Sugiura and Strangway,* 1985). The unidirectional orientation of this component requires that it was acquired after accretion on the CV parent planetesimal in a field of ~60 μT (see Fig. 7 of *Weiss and Elkins-Tanton,* 2013). This is consistent with the fact that the ferromagnetic minerals in Allende (pyrrhotite, magnetite, and awaruite) are secondary alteration products widely interpreted to have formed as a result of fluid-assisted metasomatism on the CV planetesimal (*Brearley and Krot,* 2012). Furthermore, the formation of these minerals was accompanied by or followed by thermal metamorphism to temperatures of 300°–500°C. These processes should have imprinted a thermoremanent or crystallization-remanent magnetization on the meteorite if a field was present. Although the actual age of the ferromagnetic minerals is uncertain, I/Xe thermochronometry suggests that the thermal event occurred at least 9–10 m.y. after the formation of CAIs. Because the solar nebula is only thought to have persisted for 3–6 m.y. after CAI formation, this likely postdates the existence of putative nebular magnetic fields. Therefore it was concluded that the most likely magnetic field source was an interior core dynamo, such that the CV parent body was partially differentiated with a molten metallic core and an unmelted (but variably metasomatized) relic chondritic crust (*Carporzen et al.,* 2011; *Elkins-Tanton et al.,* 2011). Dynamo generation by flow of briny fluids is extremely unlikely because of their extremely low conductivities (see *Schubert et al.,* 1996).

This proposal, which has roots in the early modern era of meteoritics, challenges the dominant view that individual planetesimals have homogenous structures that are either unmelted, partially melted throughout, or fully melted (*Weiss and Elkins-Tanton,* 2013). It proposes that planetesimals could have reached a continuum of differentiation end states that individual bodies could have restricted regions that varied in their degrees of differentiation. It therefore implies

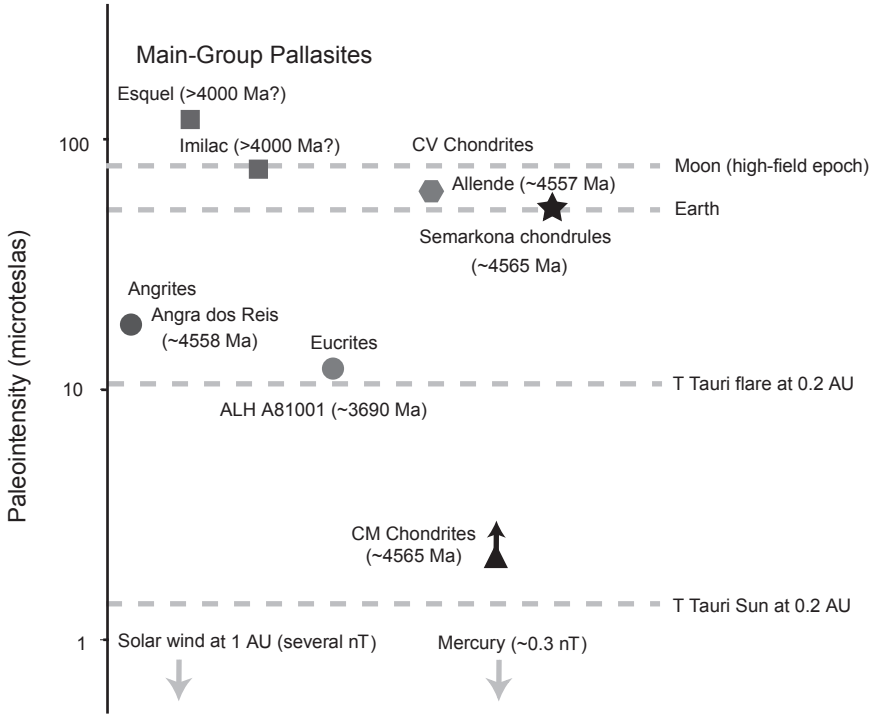

Fig. 5. Modern magnetic field paleointensity measurements from meteorites. Shown are paleointensities measured for individual meteorites from the angrite parent body, the main group pallasite parent body, the eucrite parent body, the CV chondrite parent body, and the CM chondrite parent body, all of which have been interpreted as possible records of planetesimal dynamo magnetic fields (*Weiss et al.,* 2008; *Tarduno et al.,* 2012; *Fu et al.,* 2012; *Carporzen et al.,* 2011; *Cournède et al.,* 2015). Paleointensity records of the nebular magnetic field from chondrules from the Semarkona LL ordinary chondrite (*Fu et al.,* 2014b) are shown for comparison. Also shown are the surface magnetic field on the Earth, the inferred lunar surface field from 3.56 to 3.9 Ga (*Weiss and Tikoo,* 2014), fields from the T Tauri Sun and transient flares at 0.2 AU (*Weiss et al.,* 2010a; *Vallee,* 2003), and the present-day solar wind field and surface field of Mercury (*Anderson et al.,* 2010).

that some chondrite and achondrites could have originated from a single parent body (Fig. 1). The recent identification of unidirectional magnetization in CM chondrites (*Cournède et al.,* 2015) may provide evidence for another partially differentiated chondrite parent body, although the old age of this magnetization makes it difficult to exclude an external nebular magnetic field source.

Recently, it has been proposed that the unidirectional magnetization in CV chondrites could be the product of impact-generated magnetic fields rather than a core dynamo (*Bland et al.,* 2014). In this scenario, the precursor lithologies of chondrites were heated by an impact-induced compaction event that simultaneously generated an impact plasma field, leading to the acquisition of a unidirectional thermoremanence without requiring partial differentiation. However, it is unclear whether impacts are likely to generate strong magnetic fields with sufficient duration and occurring in the appropriate location to magnetize rocks. For example, paleomagnetic studies of terrestrial craters have identified no evidence of impact-generated fields (*Weiss et al.,* 2010b). Furthermore, the peak temperatures predicted for carbonaceous meteorites by the impact-compaction hypothesis exceed the Curie temperatures of their constituent ferromagnetic minerals (pyrrhotite and magnetite, 320° and 580°C, respectively), such that the millimeter–centimeter samples studied by *Carporzen et al.* (2011) would be predicted to have magnetization blocked up to 580°C rather than the observed 290°C temperature. Finally, the ferromagnetic minerals in Allende and other CV chondrites are thought to have been produced mostly by secondary metasomatic and aqueous processes on their parent body. In particular, the presence of sulfide veins crosscutting chondrules and into the surrounding matrix (*Krot et al.,* 1998) requires that much of the ferromagnetic minerals postdate any putative compaction event and therefore could not have been magnetized in an associated impact-generated field.

4.3. Asteroidal Magnetism

Paleomagnetic studies of meteorites indicate that some asteroids could be magnetized by an internally generated dynamo (for bodies that formed advecting cores) or could acquire large-scale magnetization during accretion by torques associated with a background field in the nebula. These conclusions could be directly tested by direct measurements of remanent magnetic fields around asteroids. Because of the inverse-cube dependence of dipolar fields with distance from the field source, direct detection of asteroidal magnetic fields requires *in situ* magnetometry measurements from spacecraft. Spacecraft have attempted this thus far near six asteroids — (21) Lutetia, (243) Ida, (433) Eros, (951) Gaspra, (2867) Šteins, and (9969) Braille — but none have unambiguously detected a remanent field from these bodies (*Kivelson et al.,* 1995; *Richter et al.,* 2012). One possible exceptions is Deep Space 1's flyby of the 0.78-km-radius Q-/S-type asteroid (9969) Braille, which observed a weak (~1–2 nT) change in the ambient magnetic field upon closest approach (28 km) (*Richter et al.,* 2001). However, this field change is near the sensitivity limit of the investigation, as demonstrated by a mismatch between the measured x-component of the field and the best-fit dipole model for the asteroidal field. Another possible exception is Galileo's flyby of the 8-km-radius S-type asteroid (951) Gaspra, during which it was thought to have detected magnetic field rotations produced by interaction of the solar wind with an intrinsic asteroidal magnetic field (*Kivelson et al.,* 1993, 1995). However, it has been subsequently proposed that the observed plasma waves do not require the presence of a significant asteroidal magnetic field but could rather be explained purely by variability of the background solar wind (*Blanco-Cano et al.,* 2003).

The lack of magnetic field detections near some of these asteroids places stringent constraints on the total magnetic moments of these asteroids. In particular, if it is assumed that the asteroids are uniformly magnetized, then the inferred upper limit on the magnetizations of asteroids (21) Lutetia *(Richter et al.,* 2012) and (433) Eros (*Acuña et al.,* 2002) are below that measured for virtually all known meteorites. This means that either these asteroids are made of materials not yet recognized as meteoritic materials on Earth or, more likely, they are made of materials resembling known meteorites but that are nonunidirectionally magnetized at spatial scales exceeding that of meteorite hand samples (>10 cm) (*Wasilewski et al.,* 2002). Therefore, magnetic field measurements of asteroids do not presently support or refute the inference made from meteorite paleomagnetic studies that many asteroids, including fully melted objects and possibly also partially differentiated bodies, likely generated dynamo magnetic fields.

4.4. Meteorite Evidence for Partial Differentiation

The existence of chondrites, primitive achondrites, and achondrites indicates that at least localized regions of planetesimals either did not melt, underwent partial melting, or completely melted. These topics are extensively reviewed elsewhere in this volume (see the chapters by Wilson et al. and Scott et al.). Here we focus on meteorite evidence for partial differentiation.

As discussed in sections 2.3 and 4.3, thermal models of asteroid differentiation and paleomagnetic studies of chondrites indicate that some bodies may have partially differentiated, such that more than one of these meteorite lithologies could have formed on the same body. In fact, the recent discovery of primitive achondrites, thought to be the residues of partial melting of chondritic precursors, as a third major category of meteorite lithologies intermediate between chondrites and achondrites provides prima facie evidence for the existence of partially differentiated bodies. Moreover, there is broad consensus that the primitive achondrite group winonaites are derived from the same parent body as IAB iron meteorites (*Benedix et al.,* 2000), which demonstrates that partially differentiated bodies contained regions that experienced a large degree of melting. Three key questions that remain are how common the formation of such bodies was in the early solar system, whether they preserved chondritic crusts, and whether they formed large-scale regions of silicate and iron metallic magmas.

As reviewed extensively by *Weiss and Elkins-Tanton* (2013), affiliated chondrites and achondrites could be recognized by their isotopic compositions, cosmic-ray exposure age distributions, and/or radioisotopic impact age distribution. The chemical compositions of the achondrites should also be consistent with fractionations expected from igneous differentiation of their chondrite protoliths. Particularly strong evidence would come from the identification of chondritic and achondritic materials that share these properties and are co-located within a single polymict meteorite.

Possible examples of affiliated chondrite and achondrite groups include the H chondrites and the silicate-bearing IIE iron meteorites. The silicates in these rocks share a common oxygen isotopic composition and bulk elemental composition, while the IIE iron meteorites also contain a diversity of silicate lithologies ranging from relic chondritic fragments, to achondritic unmelted chondrites with relic chondrules, to metamorphosed chondrites, to partial melts (*Ruzicka,* 2014). A connection between enstatite chondrites, aubrites, and recently discovered primitive achondrites of enstatite chondritic parentage has long been considered (*Keil,* 2010; *Watters and Prinz,* 1979). The paleomagnetism of at least CV chondrites has been interpreted as evidence for a core dynamo (*Carporzen et al.,* 2011; *Elkins-Tanton et al.,* 2011). Oxygen and Cr isotopic data indicate strong affiliations between CV chondrites and the ungrouped basaltic achondrite Northwest Africa (NWA) 8186 (*Agee et al.,* 2014). There are also numerous "type 7" chondrites, which appear to have been heated to temperatures at or just below metal-sulfide melting (*Irving et al.,* 2005), including metamorphosed clasts within the CV breccias Mokoia and Yamato 86009 (*Jogo et al.,* 2013). Furthermore, oxygen isotopic data link the very primitive CR chondrite group to several highly metamorphosed (type 6) chondrites such as NWA 2994 as well

as to achondrites such as NWA 5131 (*Bunch et al.,* 2008; *Wittke et al.,* 2011). It would be surprising if chondrite parent bodies were heated to temperatures either just below the solidus or else above the silicate liquidus throughout their entire volumes such that virtually no intermediate partially differentiated bodies formed in between these end members.

5. CONCLUSION

There were many competing and interacting processes occurring in small bodies in early solar system history, and differences in bulk composition and accretionary history would have led to highly diverse outcomes, only a few of which may be represented in extant meteoritic and asteroidal material.

Aluminum-26 was probably the primary energy source for the heat needed to cause large-scale differentiation, while impacts caused only local melting. Progressive heating above ~200°C generated free fluids that could have been exhaled or have participated in thermal convection, although the enstatite chondrite parent bodies may have had insufficient permeability for large-scale fluid flow. Beyond 950°C, molten metal may have begun to percolate downward and form a core, although this may require even higher temperatures. The formation of a core and the fraction of the planetesimal's total metal content that would migrate there depends on the peak temperature reached and duration of heating. These factors in turn strongly depend on body size and accretion rate.

Silicate melting will commence around 1100°C. If volatiles were not already sufficiently depleted, then volatile-rich silicate melt could rise to eject or form a crust. It could also transport ^{26}Al away from the interior, cooling the body more quickly and slowing core growth. Alternatively, volatile-depleted melt would be negatively buoyant, thereby permitting the preservation of a chondritic or primitive achondritic crust over a differentiated interior.

On bodies heated sufficiently to form a magma ocean, initial fractional solidification as the magma ocean cools would produce only olivine before a high crystal fraction suppressed fractional solidification and caused bulk solidification. This explains the presence of olivine found in pallasites and its absence from the rest of the meteorite collection. It is difficult to predict how core solidification would have proceeded since the adiabat is shallow and sulfur content is the main factor determining the solidus. However, the different solidification regimes predict different locations of sulfur-rich late-crystallizing material.

Post-accretional remanent magnetization has been found in both chondrites and achondrites, and an internal dynamo is considered the likely magnetic field source. Magnetic fields have not been decisively detected on asteroids, probably because they are non-uniformly magnetized such that they have weak total magnetic moments.

Aspects of differentiation models can be further refined to make better predictions and inferences as solar system exploration continues. For example, the hypothetical process and effects of oxidation of iron in the presence of volatiles, followed by reduction as temperature rises, should be a topic of further research. Further work permitting thermal modeling of bodies rich in ice and other volatile compounds, which are particularly likely to be present in the outer solar system, would also permit greater understanding of early solar system processes.

Acknowledgments. We thank E. D. Young and B. Z. Klein for discussions that improved the manuscript.

REFERENCES

Acuña M. H., Anderson B. J., Russell C. T., Wasilewski P., Kletetschka G., Zanetti L., and Omidi N. (2002) NEAR magnetic field observations at 433 Eros: First measurements from the surface of an asteroid. *Icarus, 155,* 220–228.

Agee C. B. (1997) Melting temperatures of the Allende meteorite: Implications for a Hadean magma ocean. *Phys. Earth Planet. Inter., 100,* 41–47.

Agee C. B., Li J., Shamon M. C., and Circone S. (1995) Pressure-temperature phase diagram for the Allende meteorite. *J. Geophys. Res., 100,* 17725–17740.

Agee C. B., Muttik N., Ziegler K., McCubbin F. M., Sanborn M. E., and Yin Q.-Z. (2014) NWA 8186: An ungrouped achondrite from the CK/CV chondrite parent body. In *73rd Meteoritical Society Meeting,* Abstract #5385.

Akai J. (1992) T-T-T diagram of serpentine and saponite, and estimation of metamorphic heating degree of Antarctic carbonaceous chondrites. *Proc. NIPR Symp. Antarct. Meteorites 5th,* pp. 120–135.

Akridge G., Benoit P. H., and Sears D. W. G. (1998) Regolith and megaregolith formation of H-chondrites: Thermal constraints on the parent body. *Icarus, 132,* 185–195.

Alexander C. M. O.'D., Barber D. J., and Hutchison R. (1989) The microstructure of Semarkona and Bishunpur. *Geochim. Cosmochim. Acta, 53,* 3045–3057.

Anderson B. J. et al. (2010) The magnetic field of Mercury. *Space Sci. Rev., 152,* 307–339.

Asphaug E. (2010) Similar-sized collisions and the diversity of planets. *Chem. Erde, 70,* 199–219.

Bagdassarov N., Golabek G. J., Solferino G., and Schmidt M. W. (2009) Constraints on the Fe-S melt connectivity in mantle silicates from electrical impedance measurements. *Phys. Earth Planet. Inter., 177,* 139–146.

Baker J. A., Bizzarro M., Wittig N., Connelly J. N., and Haack H. (2005) Early planetesimal melting from an age of 4.5662 Gyr for differentiated meteorites. *Nature, 436,* 1127–1131.

Bartels K. S. and Grove T. L. (1991) High-pressure experiments on magnesian eucrite compositions — constraints on magmatic processes in the eucrite parent body. *Proc. Lunar Planet. Sci. Conf., Vol. 21,* pp. 351–365.

Bear J. (1972) *Dynamics of Fluids in Porous Media.* Dover, New York.

Benedix G. K., McCoy T. J., Keil K., and Love S. G. (2000) A petrologic study of the IAB iron meteorites: Constraints on the formation of the IAB-winonaite parent body. *Meteoritics & Planet. Sci., 35,* 1127–1141.

Benedix G. K., Haack H., and McCoy T.J. (2014) Iron and stony-iron meteorites. In *Treatise on Geochemistry, Vol. 1: Meteorites, Comets, and Planets, 2nd edition* (A. M. Davis, ed.), pp. 325–345. Elsevier, Amsterdam.

Bennett M. E. and McSween H. Y. Jr. (1996) Revised model calculations for the thermal histories of ordinary chondrite parent bodies. *Meteoritics & Planet. Sci., 31,* 783–792.

Blanco-Cano X., Omidi N., and Russell C. T. (2003) Hybrid simulations of solar wind interaction with magnetized asteroids: Comparison with Galileo observations near Gaspra and Ida. *J. Geophys. Res., 108,* 1216.

Bland P. A., Jackson M. D., Coker R. F., et al. (2009) Why aqueous alteration in asteroids was isochemical: High porosity != high permeability. *Earth Planet. Sci. Lett., 287,* 559–568.

Bland P. A., Collins G. S., Davison T. M., Abreu N. M., Ciesla F. J., Muxowrthy A. R., and Moore J. (2014) Pressure-temperature evolution of primordial solar system solids during impact-induced compaction. *Nature Commun., 5,* 5451.

Brace W. F. (1980) Permeability of crystalline and argillaceous rocks. *Intl. J. Rock Mech. Min. Sci. Geomech., 17,* 241–251.

Brearley A. J. (2006) The action of water. In *Meteorites and the Early Solar System II* (D. S. Lauretta D. S. and H. Y. McSween Jr., eds.), pp. 587–624. Univ. of Arizona, Tucson.

Brearley A. J. and Krot A. N. (2012) Metasomatism in the early solar system: The record from chondritic meteorites. In *Metasomatism and the Chemical Transformation of Rock* (D. E. Harlov and H. Austrheim, eds.), pp. 659–789. Springer-Verlag, Berlin.

Britt D. and Consolmagno G. J. (2003) Stony meteorite porosities and densities: A review of the data through 2001. *Meteoritics & Planet. Sci., 38,* 1161–1180.

Britt D. T., Yeomans D., Housen K., and Consolmagno C. (2002) Asteroid density, porosity, and structure. In *Asteroids III* (W. F. Bottke Jr. et al., eds.), pp. 485–499. Univ. of Arizona, Tucson.

Bunch T. et al. (2008) Evidence for pervasive metamorphism on the CR chondrite parent body from highly equilibrated CR6 chondrites Northwest Africa 2994 and Northwest Africa 3100. *Lunar Planet Sci. XXXIX,* Abstract #1991. Lunar and Planetary Institute, Houston.

Buseck P. R. (1977) Pallasite meteorites — mineralogy, petrology, and geochemistry. *Geochim. Cosmochim. Acta, 41,* 711–740.

Butler R. F. (1972) Natural remanent magnetization and thermomagnetic properties of Allende meteorite. *Earth Planet. Sci. Lett., 17,* 120–128.

Cameron A. G. W., Benz W., and Wasson J. T. (1990) Heating during asteroidal collisions. *Lunar Planet. Sci. XXI,* pp. 155–156. Lunar and Planetary Institute, Houston.

Carporzen L., Weiss B. P., Elkins-Tanton L. T., Shuster D. L., Ebel D. S., and Gattacceca J. (2011) Magnetic evidence for a partially differentiated carbonaceous chondrite parent body. *Proc. Natl. Acad. Sci., 108*, 6386–6389.

Castillo-Rogez J., Johnson T. V., Lee M. H., Turner N. J., Matson D. L., and Lunine J. (2009) ^{26}Al decay: Heat production and a revised age for Iapetus. *Icarus, 204,* 658–662.

Chabot N. L. (2004) Sulfur contents of the parental metallic cores of magmatic iron meteorites. *Geochim. Cosmochim. Acta, 68,* 3607–3618.

Chabot N. L. and Drake M. J. (2000) Crystallization of magmatic iron meteorites: The effects of phosphorus and liquid immiscibility. *Meteoritics & Planet. Sci., 35,* 807–816.

Chabot N. L. and Haack H. (2006) Evolution of asteroidal cores. In *Meteorites and the Early Solar System II* (D. S. Lauretta D. S. and H. Y. McSween Jr., eds.), pp. 747–771. Univ. of Arizona, Tucson.

Chambers J. E. (2010) Planetesimal formation by turbulent concentration. *Icarus, 180,* 496–513.

Chen J. H., Papanastassiou D. A., Teus M., and Huss G. R. (2013) Fe-Ni isotopic systematics in UOC QUE 97008 and Semarkona chondrules. *Lunar Planet. Sci. XLIV,* Abstract #2649. Lunar and Planetary Institute, Houston.

Christensen U. R. (2015) Iron snow dynamo models for Ganymede. *Icarus, 247,* 248–259. DOI: 10.1016/j.icarus.2014.10.024.

Ciesla F. J., Davison T. M., Collins G. S., and O'Brien D. P. (2013) Thermal consequences of impacts in the early solar system. *Meteoritics & Planet. Sci., 48,* 2559–2576.

Clayton R. N. and Mayeda T. K. (1984) The oxygen isotope record in Murchison and other carbonaceous chondrites. *Earth Planet. Sci. Lett., 67,* 151–161.

Clauser C. (1992) Permeability of crystalline rocks. *Eos Trans. AGU, 73,* 233–238.

Coradini A., Capaccioni F., Erard S., et al. (2011) The surface composition and temperature of asteroid 21 Lutetia as observed by Rosetta/VIRTIS. *Science, 334,* 492–494.

Corrigan C. M., Zolensky M. E., Dahl J., Long M., Weir J., Sapp C., and Burkett P. J. (1997) The porosity and permeability of chondritic meteorites and interplanetary dust particles. *Meteoritics & Planet. Sci., 32,* 509–515.

Cournède C., Gattacceca J., Gounelle M., Rochette P., and Weiss B. P. (2015) An early solar system magnetic field recorded in CM chondrites. *Earth Planet. Sci. Lett., 410,* 62–74.

Cuzzi J. N., Hogan R. C., and Shariff K. (2008) Towards planetesimals: Dense chondrule clumps in the protoplanetary nebula. *Astrophys. J., 687,* 1432–1447.

Davison T. M., Collins G. S., and Ciesla F. J. (2010) Numerical modeling of heating in porous planetesimal collisions. *Icarus, 208,* 468–481.

Dauphas N., Cook D. L., Sacarabany A., Frohlich C., Davis A. M., Wadhwa M., Pourmand A., Rauscher T., and Gallino R. (2008) Iron-60 evidence for early injection and efficient mixing of stellar debris in the protosolar nebula. *Astrophys. J., 686,* 560–569.

Dodd R. T. Jr. (1969) Metamorphism of the ordinary chondrites: A review. *Geochim. Cosmochim. Acta, 33,* 161–203.

Duprat J. and Tatischeff V. (2007) Energetic constraints on *in situ* production of short-lived radionuclei in the early solar system. *Astrophys. J. Lett., 617,* L69–L72.

Elkins Tanton L. T., Weiss B. P., and Zuber M. T. (2011) Chondrites as samples of differentiated planetesimals. *Earth Planet. Sci. Lett., 305,* 1–10.

Ermakov A. I., Zuber M. T., Smith D. E., Raymond C. A., Balmino G., Fu R. R., and Ivanov B. A. (2014) Constraints on Vesta's interior structure using gravity and shape models from the Dawn mission. *Icarus, 240,* 146–160.

Fabrichnaya O. B. (1999) The phase relations in the FeO-MgO-Al_2O_3-SiO_2 system: An assessment of thermodynamic properties and phase equilibria at pressures up to 30 GPa. *Calphad, 23,* 19–67.

Fish R. A., Goles G. G., and Anders E. (1960) The record in meteorites III. On the development of meteorites in asteroidal bodies. *Astrophys. J., 132,* 243–258.

Formisano M., Turrini D., Federico C., Capaccioni F., and De Sanctis M. C. (2013) The onset of differentiation and internal evolution: The case of 21 Lutetia. *Astrophys. J., 770,* 9.

Fu R. R. and Elkins-Tanton L. T. (2014) The fate of magmas in planetesimals and the retention of primitive chondritic crusts. *Earth Planet. Sci. Lett., 390,* 128–137.

Fu R. R. and Weiss B. P. (2012) Detrital remanent magnetization in the solar nebula. *J. Geophys. Res., 117,* E02003.

Fu R. R., Weiss B. P., Shuster D. L., Gattacceca J., Grove T. L., Suavet C., Lima E. A., Li L., and Kuan A. T. (2012) An ancient core dynamo in asteroid Vesta. *Science, 338,* 238–241.

Fu R. R., Hager B. H., Ermakov A. I., and Zuber M. T. (2014a) Efficient early global relaxation of asteroid Vesta. *Icarus, 240,* 133–145.

Fu R. R., Lima E. A., and Weiss B. P. (2014b) No nebular magnetization in the Allende CV carbonaceous chondrite. *Earth Planet. Sci. Lett., 404,* 54–66.

Ghosh A. and McSween H. Y. Jr. (1998) A thermal model for the differentiation of asteroid 4 Vesta, based on radiogenic heating. *Icarus, 134,* 187–206.

Ghosh A., Weidenschilling S. J., and McSween H. Y. Jr. (2001) Thermal consequences of the multizone accretion code on the structure of the asteroid belt. *Lunar Planet. Sci. XXXII,* Abstract #1760. Lunar and Planetary Institute, Houston.

Ghosh A., Weidenschilling S. J., McSween H. Y. Jr., and Rubin A. (2006) Asteroidal heating and thermal stratification of the asteroidal belt. In *Meteorites and the Early Solar System II* (D. S. Lauretta and H. Y. McSween Jr., eds.), pp. 555–566. Univ. of Arizona, Tucson.

Golabek G. J., Bourdon B., and Gerya T. V. (2014) Numerical models of the thermomechanical evolution of planetesimals: Application to the acapulcoite-lodranite parent body. *Meteoritics & Planet. Sci., 49,* 1083–1099.

Goldstein J. I., Scott E. R. D., and Chabot N. L. (2009) Iron meteorites: Crystallization, thermal history, parent bodies, and origin. *Chem. Erde, 69,* 293–325.

Gounelle M. and Meynet G. (2012) Solar system genealogy revealed by extinct short-lived radionuclides in meteorites. *Astron. Astrophys., 545,* A4.

Grimm R. E. (1985) Penecontemporaneous metamorphism, fragmentation, and reassembly of ordinary chondrite parent bodies. *J. Geophys. Res., 90,* 2022–2028.

Grimm R. E. and McSween H. Y. Jr. (1989) Water and the thermal evolution of carbonaceous chondrite parent bodies. *Icarus, 82,* 244–280.

Grimm R. E. and McSween H. Y. Jr. (1993) Heliocentric zoning of the asteroid belt by aluminum-26 heating. *Science, 259,* 653–655.

Guo W. and Eiler J. M. (2007) Temperatures of aqueous alteration and evidence for methane generation on the parent bodies of the CM chondrites. *Geochim. Cosmochim. Acta, 71,* 5565–5575.

Haack H. and Scott E. R. D. (1992) Asteroid core crystallization by inward dendritic growth. *J. Geophys. Res., 97,* 14727–14734.

Haack H. and Scott E. R. D. (1993) Chemical fractionations in group IIIAB iron meteorites — origin by dendritic crystallization of an asteroidal core. *Geochim. Cosmochim. Acta, 57,* 3457–3472.

Haack H., Rasmussen K. L., and Warren P. H. (1990) Effects of regolith/megaregolith insulation on the cooling histories of differentiated asteroids. *J. Geophys. Res., 95,* 5111–5124.

Henke S., Gail H.-P., Trieloff M., Schwarz W. H., and Kleine T. (2012) Thermal evolution and sintering of chondritic planetesimals. *Astron. Astrophys., 537,* A45.

Herbert F., Sonnett C. P., and Gaffey M. (1991) Protoplanetary thermal metamorphism: The hypothesis of electromagnetic induction in the protosolar wind. In *The Sun in Time* (C. P. Sonnett et al., eds.), pp. 710–739. Univ. of Arizona, Tucson.

Hevey P. and Sanders I. (2006) A model for planetesimal meltdown by ^{26}Al and its implications for meteorite parent bodies. *Meteoritics & Planet. Sci., 41,* 95–106.

Huss G. R., Rubin A. E., and Grossman J. N. (2006) Thermal metamorphism in chondrites. In *Meteorites and the Early Solar System II* (D. S. Lauretta and H. Y. McSween Jr., eds.), pp. 567–586. Univ. of Arizona, Tucson.

Hutchison R., Alexander C. M. O'D., and Barber D. J. (1987) The Semarkona meteorite: First recorded occurrence of smectite in an ordinary chondrite, and its implications. *Geochim. Cosmochim. Acta, 51,* 1875–1882.

Irving A. J., Bunch T. E., Rumble D., and Larson T. E. (2005) Metachondrites: Recrystallized and/or residual mantle rocks from multiple, large chondritic parent bodies. *68th Meteoritical Society Meeting,* Abstract #5218.

Jacobsen B., Yin Q.-Z., Moyniera F., Amelin Y., Krot A. N., Nagashima K., Hutcheon I. D., and Palme H. (2008) ^{26}Al-^{26}Mg and ^{207}Pb-^{206}Pb systematics of Allende CAIs: Canonical solar initial ^{26}Al/^{27}Al ratio. *Earth Planet. Sci. Lett., 272,* 353–364.

Jarosewich E. (1990) Chemical analyses of meteorites: A compilation of stony and iron meteorite analyses. *Meteoritics, 25,* 323–337.

Jogo K., Nagashima K., Hutcheon I. D., Krot A. N., and Nakamura T. (2013) Heavily metamorphosed clasts from the CV carbonaceous chondrite breccias Mokoia and Yamato 86009. *Meteoritics & Planet. Sci., 47,* 2251–2268.

Johansen A., Oishi J. S., Mac Low M.-M., Klahr H., Henning T., and Youdin A. (2007) Rapid planetesimal formation in turbulent circumstellar disks. *Nature, 448,* 1022–1025.

Jones T. D., Lebofsky L. A., Lewis J. S., and Marley M. S. (1990) The composition and origin of the C, P, and D asteroids: Water as a tracer of thermal evolution in the outer belt. *Icarus, 88,* 172–192.

Jurewicz A. J. G., Mittlefehldt D. W., and Jones J. H. (1993) Experimental partial melting of the Allende (CV) and Murchison (CM) chondrites and the origin of asteroidal basalts. *Geochim. Cosmochim. Acta, 57,* 2123–2139.

Jurewicz A. J. G., Mittlefehldt D. W., and Jones J. H. (1995) Experimental partial melting of the St. Severin (LL) and Lost City (H) chondrites. *Geochim. Cosmochim. Acta, 59,* 391–408.

Kallemeyn G. W. and Wasson J. T. (1981) The compostional classification of chondrites — I. The carbonaceous chondrite groups. *Geochim. Cosmochim. Acta, 45,* 1217–1230.

Keil K. (2010) Enstatite achondrite meteorites (aubrites) and the histories of their asteroidal parent bodies. *Chem. Erde, 70,* 295–317.

Keil K., Stöffler D., Love S. G., and Scott E. R. D. (1997) Constraints on the role of impact heating and melting in asteroids. *Meteoritics & Planet. Sci., 32,* 349–363.

Keil K., McCoy T. J., Wilson L., Barrat J. A., Rumble D., Meier M. M. M., Wieler R., and Huss G. R. (2011) A composite Fe,Ni-FeS and enstatite-forsterite-diopside-glass vitrophyre clast in the Larkman Nunatak 04316 aubrite: Origin by pyroclastic volcanism. *Meteoritics & Planet. Sci., 46,* 1719–1741.

King C. and Olson P. (2011) Heat partitioning in metal-silicate plumes during Earth differentiation. *Earth Planet. Sci. Lett., 304,* 577–586.

Kivelson M. G., Bargatze L. F., Khurana K. K., Southwood D. J., Walker R. J., and Coleman P. J. (1993) Magnetic field signatures near Galileo's closest approach to Gaspra. *Science, 261,* 331–334.

Kivelson M. G., Wang Z., Joy S., Khurana K. K., Polanskey C., Southwood D. J., and Walker R. J. (1995) Solar wind interaction with small bodies. 2. What can Galileo's detection of magnetic rotations tell us about Gaspra and Ida. *Adv. Space Res., 16,* 47–57.

Kleine T., Hans U., Irving A. J., and Bourdon B. (2012) Chronology of the angrite parent body and implications for core formation in protoplanets. *Geochim. Cosmochim. Acta, 84,* 186–203.

Kracher A. and Wasson J. T. (1982) The role of S in the evolution of the parental cores of the iron meteorites. *Geochim. Cosmochim. Acta, 46,* 2419–2426.

Krot A. N., Scott E. R. D., and Zolensky M. E. (1997) Origin of fayalitic olivine rims and lath-shaped matrix olivine in the CV3 chondrite Allende and its dark inclusions. *Meteoritics & Planet. Sci., 32,* 31–49.

Krot A. N., Petaev M. I., Scott E. R. D., Choi B.-G., Zolensky M. E., and Keil K. (1998) Progressive alteration in CV3 chondrites: More evidence for asteroidal alteration. *Meteoritics & Planet. Sci., 33,* 1065–1085.

Krot A. N., Amelin Y., Cassen P., and Meibom A. (2005) Young chondrules in CB chondrites from a giant impact in the early solar system. *Nature, 436,* 989–992.

Krot A. N., Nagashima K., Bizzarro M., Huss G. R., Davis A. M., McKeegan K. D., Meyer B. S., and Ulyanov A. A. (2008) Multiple generations of refractory inclusions in the metal-rich carbonaceous chondrites Acfer 182/214 and Isheyevo. *Astrophys. J., 672,* 713–721.

Krot A. N., Makide K., Nagashima K., Huss G. R., Ogliore R. C., Ciesla F. J., Yang L., Hellebrand E., and Gaidos E. (2012) Heterogeneous distribution of ^{26}Al at the birth of the solar system: Evidence from refractory grains and inclusions. *Meteoritics & Planet. Sci., 47,* 1948–1979.

Kullerud G. (1963) The Fe-Ni-S system. *Annu. Rept. Geophys. Lab., 1412,* 175–189.

Kullerud G. and Yoder H. S. (1959) Pyrite stability relations in the Fe-S system. *Econ. Geol., 54,* 533–572.

Kunihiro T., Rubin A. E., McKeegan K. D., and Wasson J. T. (2004) Initial ^{26}Al/^{27}Al in carbonaceous-chondrite chondrules: Too litte ^{26}Al to melt asteroids. *Geochim. Cosmochim. Acta, 68,* 2947–2957.

Laneuville M., Wieczorek M. A., Breuer D., Aubert J., Morard G., and Ruckriemen T. (2014) A long-lived lunar dynamo powered by core crystallization. *Earth Planet. Sci. Lett., 401,* 251–260.

LaTourrette T. and Wasserburg G. J. (1998) Mg diffusion in anorthite: Implications for the formation of early solar system planetesimals. *Earth Planet. Sci. Lett., 158,* 91–108.

Lee M. S., Rubin A. E., and Wasson J. T. (1992) Origin of metallic Fe-Ni in Renazzo and related chondrites. *Geochim. Cosmochim. Acta, 56,* 2521–2533.

Lee T., Papanastassiou D. A., and Wasserburg G. J. (1976) Demonstration of ^{26}Mg excess in Allende and evidence for ^{26}Al. *Geophys. Res. Lett., 3,* 41–44.

Lerner N. R. (1995) Influence of Murchison or Allende minerals on hydrogen-deuterium exchange of amino acids. *Geochim. Cosmochim. Acta, 59,* 1623–1631.

Liu M.-C., McKeegan K. D., Goswami J. N., Marhas K. K., Sahijpal S., Ireland T. R., and Davis A. M. (2009) Isotopic records in CM hibonites: Implications for timescales of mixing of isotope reservoirs in the solar nebula. *Geochim. Cosmochim. Acta, 73,* 5051–5079.

Lodders K. (2003) Solar system abundances and condensation temperatures of the elements. *Astrophys. J., 591,* 1220–1247.

Lodders K. and Fegley B. (1998) *The Planetary Scientist's Companion.* Oxford Univ., New York.

MacPherson G. J., Davis A. M., and Zinner E. K. (1995) The distribution of ^{26}Al in the early solar system: A reappraisal. *Meteoritics & Planet. Sci., 30,* 365–386.

Makide K., Nagashima K., Krot A. N., Huss G. R., Hutcheon I. D., and Bischoff A. (2009) Oxygen- and magnesium-isotope compositions of calcium-aluminum rich inclusions from CR2 carbonaceous chondrites. *Geochim. Cosmochim. Acta, 73,* 5018–5051.

Markowski A., Quitté G., Halliday A. N., and Kleine T. (2006) Tungsten isotopic compositions of iron meteorites: Chronological constraints vs. cosmogenic effects. *Earth Planet. Sci. Lett., 242,* 1–15.

Matza S. D. and Lipschutz M. E. (1977) Volatile/mobile trace elements in Karoonda (C4) chondrite. *Geochim. Cosmochim. Acta, 41,* 1398–1401.

McCoy T. J., Keil K., Muenow D. W., and Wilson L. (1997) Partial melting and melt migration in the acapulcoite-lodranite parent body. *Geochim. Cosmochim. Acta, 61,* 639–650.

McCoy T. J., Dickinson T. L., and Lofgren G. E. (1999) Partial melting of the Indarch (EH4) meteorite: A textural, chemical, and phase relations view of melting and melt migration. *Meteoritics & Planet. Sci., 34,* 735–746.

McCoy T. J., Mittlefehldt D. W., and Wilson L. (2006) Asteroid differentiation. In *Meteorites and the Early Solar System II* (D. S. Lauretta and H. Y. McSween Jr., eds.), pp. 733–745. Univ. of Arizona, Tucson.

McKenzie D. and Bickle M. J. (1988) The volume and composition of melt generated by extension of the lithosphere. *J. Petrol., 29,* 625–697.

McSween H. Y. Jr., Ghosh A., Grimm R. E., Wilson L., and Young E. D. (2002). Thermal evolution models of planetesimals. In *Asteroids III* (W. F. Bottke Jr. et al., eds.), pp. 559–571. Univ. of Arizona, Tucson.

Merk R., Breuer D., and Spohn T. (2002) Numerical modeling of ^{26}Al-induced radioactive melting of asteroids considering accretion. *Icarus, 159,* 183–191.

Mishra R. K., Goswami J. N., Tachibana S., Huss G. R., and Rudraswami N. G. (2010) ^{60}Fe and ^{26}Al in chondrules from unequilibrated chondrites: Implications for early solar system processes. *Astrophys. J. Lett., 714,* L217–L221.

Mittlefehldt D. W., McCoy T. J., Goodrich C. A., and Kracher A. (1998) Non-chondritic meteorites from asteroidal bodies. *Rev. Mineral., 36,* D1–D195.

Miyamoto M. (1991) Thermal metamorphism of CI and CM carbonaceous chondrites: An internal heating model. *Meteoritics, 26,* 111–115.

Morbidelli A., Nesvorný D., Bottke W. F., and Levison H. F. (2009) Asteroids were born big. *Icarus, 204,* 558–573.

Moskovitz N. and Gaidos E. (2011) Differentiation of planetesimals and the thermal consequences of melt migration. *Meteoritics & Planet. Sci., 46,* 903–918.

Moskovitz N. and Walker R. J. (2011) Size of the group IVA iron meteorite core: Constraints from the age and composition of Muonionalusta. *Earth Planet. Sci. Lett., 308,* 410–416.

Muenow D. W., Keil K., and Wilson L. (1992) High-temperature mass spectrometric degassing of enstatite chondrites: Implications for pyroclastic volcanism on the aubrite parent body. *Geochim. Cosmochim. Acta, 56,* 4267–4280.

Muenow D. W., Keil K., and McCoy T. J. (1995) Volatiles in unequilibrated ordinary chondrites: Abundances, sources and implications for explosive volcanism on differentiated asteroids. *Meteoritics & Planet. Sci., 30,* 639–645.

Nagata T. and Funaki M. (1983) Paleointensity of the Allende carbonaceous chondrite. *Mem. Natl. Inst. Polar Res., Spec. Issue 30,* 403–434.

Narayan C. and Goldstein J. I. (1982) A dendritic solidification model to explain Ge-Ni variations in iron meteorite chemical groups. *Geochim. Cosmochim. Acta, 46,* 259–268.

Neumann W., Breuer D., and Spohn T. (2012) Differentiation and core formation in accreting planetesimals. *Astron. Astrophys., 543,* A141.

Neumann W., Breuer D., and Spohn T. (2014) Differentiation of Vesta: Implications for a shallow magma ocean. *Earth Planet. Sci. Lett., 395,* 267–280.

Niida K. and Green D. H. (1999) Stability and chemical composition of pargasitic amphibole in MORB pyrolite under upper mantle conditions. *Contrib. Mineral Petrol., 135,* 18–40.

Norris T. L., Gancarz A. J., Rokop D. J., and Thomas K. W. (1983) Half-life of ^{26}Al. *Proc. Lunar Planet. Sci. Conf. 14th,* in *J. Geophys. Res., 88,* B331–B333.

Pernicka E. and Wasson J. T. (1987) Ru, Re, Os, Pt and Au in iron meteorites. *Geochim. Cosmochim. Acta, 51,* 1717–1726.

Richter I., Brinza D. E., Cassel M., Glassmeier K.-H., Kuhnke F., Musmann G., Othmer C., Schwingenschuh K., and Tsurutani B. T. (2001) First direct magnetic field measurements of an asteroidal magnetic field: DS1 at Braille. *Geophys. Res. Lett., 28,* 1913–1916.

Richter I., Auster H. U., Glassmeier K.-H., Koenders C., Carr C. M., Motschmann U., Müller J., and McKenna-Lawlor S. (2012) Magnetic field measurements during the Rosetta flyby at asteroid (21) Lutetia. *Planet. Space Sci., 66,* 155–164.

Rivkin A. S., Howell E. S., Vilas F., and Lebofsky L. A. (2002) Hydrated minerals on asteroids: The astronomical record. In *Asteroids III* (W. F. Bottke Jr. et al., eds.), pp. 235–254. Univ. of Arizona, Tucson.

Rubin A. E. (1995) Petrologic evidence for collisional heating of chondritic asteroids. *Icarus, 113,* 156–167.

Rubin A. E. (2004) Postshock annealing and postannealing shock in equilibrated ordinary chondrites: Implications for the thermal and shock histories of chondritic asteroids. *Geochim. Cosmochim. Acta, 68,* 673–689.

Rubin A. E. and Jones R. H. (2003) Spade: An H chondrite impact-melt breccia that experienced post-shock annealing. *Meteoritics & Planet. Sci., 38,* 1507–1520.

Rugel G., Faestermann T., Knie K., Korschinek G., Poutivtsev M., Schumann D., Kivel N., Gunther-Leopold I., Weinreich R., and Wholmuther M. (2009) New measurement of the ^{60}Fe half-life. *Phys. Rev. Lett., 103,* 1–4.

Russell C. T., Raymond C. A., Coradini A., et al. (2012) Dawn at Vesta: Testing the protoplanetary paradigm. *Science, 336,* 684–686.

Ruzicka A. (2014) Silicate-bearing iron meteorites and their implications for the evolution of asteroidal parent bodies. *Chem. Erde, 74,* 3–48.

Sahijpal S. and Goswami J. N. (1998) Refractory phases in primitive meteorites devoid of ^{26}Al and ^{41}Ca: Representative samples of first solar system solids? *Astrophys. J. Lett., 509,* L137–L140.

Sahijpal S. and Gupta G. (2011) Did the carbonaceous chondrites evolve in the crustal regions of partially differentiated asteroids? *J. Geophys. Res., 116,* E06004.

Sahijpal S., Soni P., and Gupta G. (2007) Numerical simulations of the differentiation of accreting planetesimals with ^{26}Al and ^{60}Fe as the heat sources. *Meteoritics & Planet. Sci., 42,* 1529–1548.

Schölling M. and Breuer D. (2009) Numerical simulation of convection in a partially molten planetesimal. *Proc. European Planet. Sci. Congress 4th,* p. 523.

Scott E. R. D., Keil K. and Stöffler D. (1992) Shock metamorphism of carbonaceous chondrites. *Geochim. Cosmochim. Acta, 56,* 4281–4293.

Scott E. R. D., Love S. G., and Krot A. N. (1996a) Formation of chondrules and chondrites in the protoplanetary nebula. In *Chondrules and the Protoplanetary Disk* (R. H Hewins et al., eds.), pp. 87–96. Cambridge Univ., Cambridge.

Scott E. R. D., Haack H., and McCoy T. J. (1996b) Core crystallization and silicate-metal mixing in the parent body of the IVA iron and stony-iron meteorites. *Geochim. Cosmochim. Acta, 60,* 1615–1631.

Schubert G., Zhang K., Kivelson M. G., and Anderson J. D. (1996) The magnetic field and internal structure of Ganymede. *Nature, 384,* 544–545.

Sengers J. V. and Kamgar-Parsi B. (1984) Representative equations for the viscosity of water substance. *J. Phys. Chem. Ref. Data, 13,* 185–205.

Sharp T. G. and De Carli P. G. (2006) Shock effects in meteorites. In *Meteorites and the Early Solar System II* (D. S. Lauretta and H. Y. McSween Jr., eds.), pp. 653–677. Univ. of Arizona, Tucson.

Shepard M. K., Clark B. E., Ockert-Bell M., Nolan M. C., Howell E. S., Magri C., Giorgini J. D., Benner L. A. M., Ostro S. J., Harris A. W., Warner J. L., Stephens R. D., and Mueller M. (2010) A radar survey of M- and X-class asteroids II. Summary and synthesis. *Icarus, 208,* 221–237.

Smits P. J., Economou I. G., Peters C. J., and Arons J. S. (1994) Equation of state description of thermodynamics properties of near-critical and supercritcal water. *J. Phys. Chem., 98,* 12080–12085.

Solomatov V. S. (2000) Fluid dynamics of a terrestrial magma ocean. In *Origin of the Earth and Moon* (R. M. Canup and K. Righter, eds.), pp. 323–338. Univ. of Arizona, Tucson.

Sonnett C. P. and Colburn D. S. (1968) The principle of solar wind induced planetary dynamos. *Phys. Earth Planet. Inter., 1,* 326–346.

Sonnett C. P., Colburn D. S. and Schwartz K. (1968) Electrical heating of meteorite parent bodies and planets by dynamo induction from a pre-main sequence T Tauri "solar wind". *Nature, 219,* 924–926.

Šrámek O., Milelli L., Ricard Y., and Labrosse S. (2012) Thermal evolution and differentiation of planetesimals and planetary embryos. *Icarus, 217,* 339–354.

Sterenborg M. G. and Crowley J. W. (2013) Thermal evolution of early solar system planetesimals and the possibility of sustained dynamos. *Phys. Earth Planet. Inter., 214,* 53–73.

Stevenson D. J. (1981) Models of the Earth's core. *Science, 214,* 611–619.

Suckale J., Elkins-Tanton L. T., and Sethian J. A. (2012) Crystals stirred up: 2. Numerical insights into the formation of the earliest crust on the Moon. *J. Geophys. Res., 117,* E08005.

Sugiura N. and Strangway D. W. (1985) NRM directions around a centimeter-sized dark inclusion in Allende. *Proc. Lunar Planet. Sci. Conf. 15th,* in *J. Geophys. Res., 90,* C729–C738.

Sugiura N., Brar N. S., and Strangway D. W. (1984) Degassing of meteorite parent bodies. *Proc. Lunar Planet. Sci. Conf. 14th,* in *J. Geophys. Res., 89,* B641–B644.

Tachibana S., Huss G. R., Kita N. T., Shimoda G., and Morishita Y. (2006) ^{60}Fe in chondrites: Debris from a nearby supernova in the early solar system? *Astrophys. J. Lett., 639,* L87–L90.

Tang H. and Dauphas N. (2012) Abundance, distribution, and origin of ^{60}Fe in the solar protoplanetary disk. *Earth Planet. Sci. Lett., 359,* 248.
Tarduno J. A. and Cottrell R. D. (2012) Single crystal paleointensity analyses of olivine-diogenites: Implications for a past Vestan dynamo. *Lunar Planet Sci. XLIII,* Abstract #2663. Lunar and Planetary Institute, Houston.
Tarduno J. A., Cottrell R. D., Nimmo F., Hopkins J., Voronov J., Erickson A., Blackman E., Scott E. R. D., and McKinley R. (2012) Evidence for a dynamo in the main group pallasite parent body. *Science, 338,* 939–942.
Terasaki H., Frost D. J., Rubie D. C., and Langenhorst F. (2008) Percolative core formation in planetesimals. *Earth Planet. Sci. Lett., 273,* 132–137.
Trimmer D., Bonner B., Heard H. C., and Duba A. (1980) Effect of pressure and stress on water transport in intact and fractured gabbro and granite. *J. Geophys. Res., 85,* 7059–7071.
Ulff-Møller F., Choi B. G., Rubin A. E., Tran J., and Wasson J. T. (1998) Paucity of sulfide in a large slab of Esquel: New perspectives on pallasite formation. *Meteoritics & Planet. Sci., 33,* 221–227.
Urey H. C. (1955) The cosmic abundances of potassium, uranium, and thorium and the heat balance of the Earth, the Moon, and Mars. *Proc. Natl. Acad. Sci., 41,* 127–144.
Vallée J. P. (2003) Astral magnetic fields as observed in star-forming nurseries, in stars, and in the solar system. *New Astron. Rev., 47,* 85–168.
Van Schmus W. R. and Wood J. A. (1967) A chemical-petrologic cassification for the chondritic meteorites. *Geochim Cosmochim. Acta, 31,* 747–765.
Vernazza P., Lamy P., Groussin O., Hiroi T., Jorda L., King P. L., Izawa M. R. M., Marchis F., Birlan M., and Brunetto R. (2011) Asteroid (21) Lutetia as a remnant of Earth's precursor planetesimals. *Icarus, 216,* 650–659.
Wasilewski P., Acuña M. H., and Kletetschka G. (2002) 433 Eros: Problems with the meteorite magnetism record in attempting an asteroid match. *Meteoritics & Planet. Sci., 37,* 937–950.
Wasson J. T. (1999) Trapped melt in IIIAB irons: Solid/liquid elemental partitioning during the fractionation of the IIIAB magma. *Geochim. Cosmochim. Acta, 63,* 2875–2889.
Wasson J. T. and Richardson J. W. (2001) Fractionation trends among IVA iron meteorites: Contrasts with IIIAB trends. *Geochim. Cosmochim. Acta, 65,* 951–970.
Wasson J. T., Rubin A. E., and Benz W. (1987) Heating of primitive, asteroid-size bodies by large impacts. *Meteoritics, 22,* 525–526.
Watters T. R. and Prinz M. (1979) Aubrites: Their origin and relationship to enstatite chondrites. *Proc. Lunar Planet. Sci Conf. 10th,* pp. 1073–1093.
Webster J. D. (1997) Chloride solubility in felsic melts and the role of chloride in magmatic degassing. *J. Petrol., 38,* 1793–1807.
Weiss B. P. and Elkins-Tanton L. T. (2013) Differentiated planetesimals and the parent bodies of chondrites. *Annu. Rev. Earth Planet. Sci., 41,* 529–560.
Weiss B. P. and Tikoo S. M. (2014) The lunar dynamo. *Science, 346,* 1246753.
Weiss B. P., Berdahl S., Elkins-Tanton L. T., Stanley S., Lima E. A., and Carporzen L. (2008) Magnetism on the angrite parent body and the early differentiation of planetesimals. *Science, 322,* 713–716.
Weiss B. P., Gattacceca J., Stanley S., Rochette P., and Christensen U. R. (2010a) Paleomagnetic records of meteorites and early planetesimal differentiation. *Space Sci. Rev., 152,* 341–390.
Weiss B. P., Pedersen S., Garrick-Bethell I., Stewart S. T., Louzada K. L., Maloof A. C., and Swanson-Hysell N. L. (2010b) Paleomagnetism of impact spherules from Lonar crater, India and a test for impact-generated fields. *Earth Planet. Sci. Lett., 298,* 66–76.
Weiss B. P., Elkins-Tanton L. T., Barucci M. A., et al. (2012) Possible evidence for partial differentiation of asteroid Lutetia from Rosetta. *Planet. Space Sci., 66,* 137–146.
Williams Q. (2009) Bottom-up versus top-down solidification of the cores of small solar system bodies: Constraints on paradoxical cores. *Earth Planet. Sci. Lett., 284,* 564–569.
Willis J. and Goldstein J. I. (1982) The effects of C, P, and S on trace-element partitioning during solidification in Fe-Ni alloys. *Proc. Lunar Planet. Sci. Conf. 13th,* in *J. Geophys. Res., 87,* A435–A445.
Wilson L. and Keil K. (1991) Consequences of explosive eruptions on small solar system bodies: The case of the missing basalts on the aubrite parent body. *Earth Planet. Sci. Lett., 104,* 505–512.
Wilson L. and Keil K. (1997) The fate of pyroclasts produced in explosive eruptions on the asteroid 4 Vesta. *Meteoritics & Planet. Sci., 32,* 813–823.
Wilson L. and Keil K. (2000) Crust development on differentiated asteroids. *Lunar Planet. Sci. XXXI,* Abstract #1576. Lunar and Planetary Institute, Houston.
Wilson L. and Keil K. (2012) Volcanic activity on differentiated asteroids: A review and analysis. *Chem. Erde, 72,* 289–321.
Wilson L., Keil K., Browning L. B., Krot A. N., and Bourcher W. (1999) Early aqueous alteration, explosive disruption, and reprocessing of asteroids.. *Meteoritics & Planet. Sci., 34,* 541–557.
Wilson L., Goodrich C. A., and Van Orman J. A. (2008) Thermal evolution and physics of melt extraction on the ureilite parent body. *Geochim. Cosmochim. Acta, 72,* 6154–6176.
Wilson L., Keil K., and McCoy T. J. (2010) Pyroclast loss or retention during explosive volcanism on asteroids: Influence of asteroid size and gas content of melt. *Meteoritics & Planet. Sci., 45,* 1284–1301.
Windmark F., Birnstiel T., Ormel C. W., and Dullemond C. P. (2012) Breaking through: The effects of a velocity distribution on barriers to dust growth. *Astron. Astrophys., 544,* L16.
Wittke J. H., Bunch T. E., Irving A. J., Rumble D., and Sipiera P. P. (2011) Northwest Africa 5131: Another Tafassasset-like metachondrite related to the CR chondrite parent body. *74th Meteoritical Society Meeting,* Abstract #5222.
Wood J. A. (1962) Metamorphism in chondrites. *Geochim. Cosmochim. Acta, 26,* 739–749.
Yoshino T., Walter M. J., and Katsura T. (2003) Core formation in planetesimals triggered by permeable flow. *Nature, 422,* 154–157.
Yoshino T., Walter M. J., and Katsura T. (2004) Connectivity of molten Fe alloy in peridotite based on in situ electrical conductivity measurements: Implications for core formation in terrestrial planets. *Earth Planet. Sci. Lett., 222,* 501–516.
Young E. D. (2001) The hydrology of carbonaceous chondrite parent bodies and the evolution of planet progenitors. *Philos. Trans. R. Soc. London Ser. A, 359,* 2095–2110.
Young E. D., Ash R. D., England P., and Rumble D. III (1999) Fluid flow in chondrite parent bodies: Deciphering the compositions of planetesimals. *Science, 286,* 1331–1335.
Young E. D., Zhang K., and Schubert G. (2003) Conditions for pore water convection within carbonaceous chondrite parent bodies: Implications for planetesimal size and heat production. *Earth Planet. Sci. Lett., 213,* 249–259.
Zolensky M. E., Bourcier W. L., and Gooding J. L. (1989) Aqueous alteration on the hydrous asteroids: Results of EQ3/6 computer simulations. *Icarus, 78,* 411–425.